

We are thankful to the editor and the two reviewers for their further comments on this manuscript. Following the reviewer's suggestions, we have revised the manuscript accordingly. Listed below are our point-point responses in blue to each reviewer's comments.

In addition, a marked-up version of the manuscript was attached after the response to the reviewers' comments.

Response to Editor's comments

You have addressed the issues raised by the referees and the paper has significantly improved. The referees have given some more suggestions for technical corrections (see the referee's reports). I also have a few points here:

a) Line 120: Waliguan is one the global baseline station, so please change "regional background" to "global baseline".

Changed.

b) Line 151: please give details of the biomass burning events.

A more detailed description of the biomass burning events was added. Now it reads "There are no strong local anthropogenic source emissions in this area (~ 741 km² with a population of ~2000) except occasional biomass burning events due to burning of a large amount of straws in the middle of September and cow dung at the end of the campaign (Li et al., 2015)."

c) Line 181: give the models of these analyzers.

The models of gas analyzers were added in the revised manuscript.

"Other collocated measurements included CO by a non-dispersive infrared analyser (M300EU), O₃ by a UV photometric analyzer (Teledyne Instruments, Model 400EU), NO_x by a commercial chemiluminescence analyzer (M200EU), and SO₂ by a pulsed UV fluorescence analyzer (M100EU) and black carbon (BC) by an Aethalometer (AE31, Magee Scientific Corp)."

d) Lines 234 and 288: change "the NBS" to "the Menyuan NBS". There are some other NBS sites.

Changed.

e) Lines 317-318: Fig. 4c indicates than some factors other than boundary layer height might play an important role in the diurnal cycle of CO.

Right. Biomass burning might also affect the diurnal cycle of CO. As shown in Figure S5, biomass burning emitted a considerable amount of CO.

f) Line 325: delete "secondary". Almost all nitrate in the PM is secondary.

Deleted.

g) Libe386: change "Fig. 5b and 6" to "Figs. 5b and 6" or "Fig. 6".

Changed.

Response to Reviewer #1

The manuscript entitled, "Chemical characterization of submicron aerosol and particle growth events at a National Background Site (3295 m a. s. l.) on the Tibetan Plateau" by W. Du et al., presents non-refractory plus black carbon (BC) aerosol chemical composition and particle size distribution data from a remote location on the northeastern region of the Tibetan Plateau. This paper is of interest to many readers of Atmospheric Chemistry and Physics and it is important that it is published there. The authors put much effort and care into responding to the first round of reviewers' comments. The manuscript has improved with this revision. Thank you for making many changes and thank you to the other reviewer for focusing on details that I did not address.

It is apparent that my suggestion to provide an analysis of air mass histories at the site is beyond the scope of this manuscript. The assertion that the air was regionally-transported to the site was not backed by more information on how air was actually getting there on average. Hopefully, data from this paper will be analyzed further by someone who can study the large scale modeling and meteorology. Overall, the manuscript is pretty close to being ready to publish in ACP.

We appreciate the reviewer's constructive comments that help improve the manuscript, and we also thank the reviewer's understanding. We agree with the reviewer that the current analysis is not adequate enough to have a full understanding of the aerosol chemistry at the Menyuan national background site. We are also looking forward to further analysis by the people who are interested in this work.

To help put these results in a broader context and make it easier for the global atmospheric community to use, I strongly recommend some simple changes be incorporated into the present manuscript.

1) In lieu of an analysis of air mass histories in the present paper, it would be extremely helpful if there is a paper discussing the meteorology at the site that could be referenced in section 2.1 or perhaps references to other measurements that have been taken at the site in the past, if available.

We thank the reviewer's suggestions. This is the first time to report the measurements and the results at the Menyuan national background site. There are no references to discuss the meteorology and measurements at this site yet.

2) The maps in Figs. 1 and S3 do not show scales - for example, how many km are represented in each of them? Please add that information.

The scale of the map was added in Figure 1 and Figure S3 in the revised manuscript.

3) For Figure 1, please add to the caption text that the pie charts show data from AMS (non-refractory composition only) plus black carbon. Also, please add to the caption an explanation for the dotted blue lines. Along the same lines, please

indicate in the caption for table S1 that all the measurements were using an AMS and in some cases with black carbon.

Thank the reviewer's comments. Figure 1 and Table S1 was revised according to the reviewer's suggestions.

"Figure 1. Map of the sampling site (Menyuan, Qinghai). Also shown is the chemical composition of submicron aerosols (NR-PM₁ + BC if it was available) measured at selected rural/remote sites in East Asia except Lanzhou, an urban site in northwest China. The two dotted blue lines are used to guide eyes for the three rural/remote regions from the west to the east. The detailed information of the sampling sites is presented in Table S1."

"Table S1. A summary of mass concentration and composition of NR-PM₁ species measured by the AMS and in some cases with black carbon (BC) at different locations in East Asia."

4) Please put the two altitude profiles of the back trajectories back into the SI, along with an indication of where Xining is on the "Clean 1" trajectory of altitude as function of time back. Please add a note in the caption that the black line is ground level, if that is what it means.

We thank the reviewer's comments. The altitude profiles of the back trajectories were added in Figure S3 in the revised manuscript.

5) The diurnal plots of the meteorological data in the SI are very important, especially when combined with the aerosol and gas phase measurements. The winds appear to be changing from the west to from the south, just at the time that the new particles are detected. If possible, it would be worthwhile to classify these air mass histories. This could be important in further interpreting the new particle formation events.

We thank the reviewer's comments. We also noticed such a change. However, the diurnal cycle of wind direction showed a large variation (25%-75% percentile, > 100°) during this period of time. In addition, we didn't observe a clear wind direction change between 8:00 – 10:00 based on the time series of meteorological variables in Figure 3. For these reasons, it is difficult to link new particle formation events to the change of wind direction.

6) The building was at a higher temperature than ambient and the air sampled by the instrument was in the inlet for about 5 seconds. Please add a comment in the text on the how much ammonium nitrate (and other semi-volatile species) could have evaporated before sampling. Could this be another reason why nitrate levels were lower for the present study compared to sites in eastern China?

The loss of ammonium nitrate and other semi-volatile species at 23 °C were small based on the thermodenuder measurements (Huffman et al., 2009). In addition, most of previous AMS measurements in China were conducted under the similar room conditions, i.e., 23-25°C air conditioned room or trailers. Therefore, the lower

nitrate concentration level at Menyuan site was not likely due to the evaporative loss of ammonium nitrate.

7) I respectfully disagree with the authors' choice of units for the aerosol mass and number concentrations in the present paper. I understand that previous data from the region was reported for ambient conditions and that the present results are reported for ambient conditions for consistency. It is unfortunate that the prior data from this region were not reported for standard conditions, especially since some sites are very high in altitude. Also, I realize that converting the current data into standard units is somewhat trivial if the ambient conditions are also reported (here sampling temperature was about 23 degrees C and the ambient pressure was not reported and is not readily apparent). However, when working with data sets at pressures significantly different from standard conditions (such as high altitude or aircraft data or global/regional modeling results and comparing the current results to sites at sea level like most listed in Figure 1 and Table S1), it is significantly easier to compare data if it is all reported using standard conditions. Because the site was relatively high in altitude (3295 m a. s. l.), the ambient pressure is roughly 0.67 times sea level pressure, resulting in a correction of a factor of 1.5. Correcting for sampling temperature to standard temperature of 273.15 K will be another factor of 1.08. Please clearly add a sentence (or a two) in the text that mentions the conversion to standard units is roughly a factor of 1.6 (or the average for the ambient conditions), so that the data reported for standard conditions can be quickly estimated if needed.

We thank the reviewer's comments. The average pressure during this study period is 695.4 hPa, and the average ambient air temperature is 4.9 °C (-8.7 - 17.9°C), so the conversion factor to standard units is roughly 1.5. Following the reviewer's suggestion, a sentence was added in Section 2.2.

"All the data are reported at ambient conditions in Beijing Standard Time. Note that the concentrations would be a factor of approximately 1.5 of the current values if the data are converted to mass loadings at standard temperature and pressure (STP, 273K and 1013.25 hPa)."

8) I also respectfully disagree with the authors' choice of units for the gas phase species. While it may be convenient for aerosol scientists to report gas phase data in micrograms per cubic meter, these units for gas phase species are not commonly used in atmospheric science and gas phase data are virtually always reported as volume mixing ratios (and what does micrograms per cubic meter mean for NOx?). Again, it is difficult to compare the data reported in this paper without recalculating the gas phase data into units of mixing ratio – for the species here "ppbv" is the most convenient. Please convert all reported gas phase data into mixing ratios of ppbv and change them in the figures and tables.

We thank the reviewer's comments. Following the reviewer's suggestions, all gas phase data were converted to volume mixing ratios using Eq. (1).

$$C = \frac{22.4 \times 101.325 \times (273 + T)}{M \times P \times 273} X \quad (1)$$

Where C is the volume mixing ratio, X is the mass concentration in $\mu\text{g m}^{-3}$, M is the molecular weight of gas species, and P and T refer to the pressure and temperature, respectively.

Response to Reviewer #2

General comments:

I found the resubmitted paper much easier to read, and several of my comments were addressed in sufficient detail. Many thanks for your revised manuscript, which I am happy to accept for publication subject to a few minor revisions as detailed below.

Specific comments:

Line 223-232: I would like to suggest the author to add the sampling year in each citation. Specify/remind readers that these comparisons are for different year.

Good point. The sampling year for each citation was added in the new version of the manuscript.

“Okinawa ($14.5 \mu\text{g m}^{-3}$) (Zhang et al., 2007) and Fukue ($12.0 \mu\text{g m}^{-3}$) (Takami et al., 2005) in Japan in 2003, and Jeju ($8.6 \mu\text{g m}^{-3}$) in Korea in 2001 (Topping et al., 2004), it is much higher than those reported at rural/remote sites in north America and Europe, e.g., Chebogue ($2.9 \mu\text{g m}^{-3}$), Storm Peak in 2004 ($2.1 \mu\text{g m}^{-3}$) and Hyytiälä in 2005 ($2.0 \mu\text{g m}^{-3}$), and even comparable to the loadings at urban sites, e.g., New York City in 2004 ($12 \mu\text{g m}^{-3}$), Pittsburgh ($15 \mu\text{g m}^{-3}$), and Manchester in 2002 ($14.0 \mu\text{g m}^{-3}$) (Zhang et al., 2007).”

Line 325: secondary nitrate --> nitrate

Changed.

References:

- Huffman, J. A., Docherty, K. S., Aiken, A. C., Cubison, M. J., Ulbrich, I. M., DeCarlo, P. F., Sueper, D., Jayne, J. T., Worsnop, D. R., Ziemann, P. J., and Jimenez, J. L.: Chemically-resolved aerosol volatility measurements from two megacity field studies, *Atmos. Chem. Phys.*, 9, 7161-7182, 2009.
- Takami, A., Miyoshi, T., Shimono, A., and Hatakeyama, S.: Chemical composition of fine aerosol measured by AMS at Fukue Island, Japan during APEX period, *Atmos. Environ.*, 39, 4913-4924, 2005.
- Topping, D., Coe, H., McFiggans, G., Burgess, R., Allan, J., Alfarra, M. R., Bower, K., Choularton, T. W., Decesari, S., and Facchini, M. C.: Aerosol chemical characteristics from sampling conducted on the Island of Jeju, Korea during ACE Asia, *Atmospheric Environment*, 38, 2111-2123, 10.1016/j.atmosenv.2004.01.022, 2004.
- Zhang, Q., Jimenez, J. L., Canagaratna, M. R., Allan, J. D., Coe, H., Ulbrich, I., Alfarra, M. R., Takami, A., Middlebrook, A. M., Sun, Y. L., Dzepina, K., Dunlea, E., Docherty, K., DeCarlo, P. F., Salcedo, D., Onasch, T., Jayne, J. T., Miyoshi, T., Shimono, A., Hatakeyama, S., Takegawa, N., Kondo, Y., Schneider, J., Drewnick, F., Borrmann, S.,

Weimer, S., Demerjian, K., Williams, P., Bower, K., Bahreini, R., Cottrell, L., Griffin, R. J., Rautiainen, J., Sun, J. Y., Zhang, Y. M., and Worsnop, D. R.: Ubiquity and dominance of oxygenated species in organic aerosols in anthropogenically-influenced Northern Hemisphere midlatitudes, *Geophysical Research Letters*, 34, L13801, 10.1029/2007gl029979, 2007.

1 Chemical Characterization of Submicron Aerosol and Particle Growth
2 Events at a National Background Site (3295 m a.s.l.) on the Tibetan
3 Plateau

4
5 W. Du^{1,2}, Y. L. Sun^{1,*}, Y. S. Xu³, Q. Jiang¹, Q. Q. Wang¹, W. Yang³, F. Wang³, Z. P.
6 Bai³, X. D. Zhao⁴, and Y. C. Yang²

7
8 ¹*State Key Laboratory of Atmospheric Boundary Layer Physics and Atmospheric Chemistry,*
9 *Institute of Atmospheric Physics, Chinese Academy of Sciences, Beijing 100029, China*

10 ²*Department of Resources and Environment, Air Environmental Modeling and Pollution*
11 *Controlling Key Laboratory of Sichuan Higher Education Institutes, Chengdu University of*
12 *Information Technology, Chengdu 610225, China*

13 ³*Chinese Research Academy of Environmental Sciences, Beijing 100012, China*

14 ⁴*National Station for Background Atmospheric Monitoring, Menyuan, Qinghai 810000,*
15 *China*

16
17
18 *Correspondence to: Y. L. Sun (sunyele@mail.iap.ac.cn)

19 **Abstract**

20 Atmospheric aerosols exert highly uncertain impacts on radiative forcing and also
21 have detrimental effects on human health. While aerosol particles are widely
22 characterized in megacities in China, aerosol composition, sources and particle
23 growth in rural areas in the Tibetan Plateau remain less understood. Here we present
24 the results from an autumn study that was conducted from 5 September to 15 October
25 2013 at a national background monitoring station (3295 m a.s.l.) in the Tibetan
26 Plateau. The submicron aerosol composition and particle number size distributions
27 were measured in situ with an Aerodyne Aerosol Chemical Speciation Monitor
28 (ACSM) and a Scanning Mobility Particle Sizer (SMPS). The average mass
29 concentration of submicron aerosol (PM₁) is 11.4 μg m⁻³ (range: 1.0 - 78.4 μg m⁻³) for
30 the entire study, which is much lower than those observed at urban and rural sites in
31 eastern China. Organics dominated PM₁ on average accounting for 43%, followed by
32 sulfate (28%) and ammonium (11%). Positive matrix factorization analysis of ACSM
33 organic aerosol (OA) mass spectra identified an oxygenated OA (OOA) and a biomass
34 burning OA (BBOA). The OOA dominated OA composition accounting for 85% on
35 average, 17% of which was inferred from aged BBOA. The BBOA contributed a
36 considerable fraction of OA (15%) due to the burning of cow dung and straws in
37 September. New particle formation and growth events were frequently observed (80%
38 of time) throughout the study. The average particle growth rate is 2.0 nm hr⁻¹ (range:
39 0.8 – 3.2 nm hr⁻¹). By linking the evolution of particle number size distribution to
40 aerosol composition, we found an elevated contribution of organics during particle
41 growth periods and also a positive relationship between the growth rate and the
42 fraction of OOA in OA, which potentially indicates an important role of organics in
43 particle growth in the Tibetan Plateau.

44

45 **Keywords**

46 **Tibetan Plateau; ACSM; Submicron Aerosol; OOA; BBOA; Particle Growth**

47 **1 Introduction**

48 High concentration of atmosphere aerosol associated with the rapid economic
49 growth, urbanization and industrialization has become a major environmental concern
50 in China. Aerosol particles especially fine particles (PM_{2.5}) have large impacts on
51 human health, natural ecosystem, weather and climate, radiative balance and the
52 self-purification capacity of troposphere (Jacobson, 2001; Tie and Cao, 2009). As a
53 result, a large number of studies have been conducted to investigate the sources,
54 chemical and physical properties, and evolution processes of aerosol particles at urban
55 and rural sites in China during the last decade (Cao et al., 2007; Wu et al., 2007; He et
56 al., 2011; Gong et al., 2012; Huang et al., 2012; Huang et al., 2013; Sun et al., 2013;
57 Jiang et al., 2015). The results showed that fine particles are mainly composed of
58 organics, sulfate, nitrate, ammonium, mineral dust, and black carbon. The sources of
59 organic aerosol (OA) were also characterized and various OA factors from distinct
60 sources were identified including primary OA (POA), e.g., hydrocarbon-like OA
61 (HOA), cooking OA (COA), biomass burning OA (BBOA) and coal combustion OA
62 (CCOA), and secondary OA (SOA), e.g., semi-volatile oxygenated OA (SV-OOA)
63 and low volatility OOA (LV-OOA) (Huang et al., 2010; Sun et al., 2010; He et al.,
64 2011; Huang et al., 2011; Xu et al., 2014a; Sun et al., 2014). While previous studies
65 significantly improve our understanding on the sources and chemical properties of
66 aerosol particles, they were mainly conducted in developed areas in China, including
67 Beijing-Tianjin-Hebei, Pearl River Delta and Yangtze River Delta.

68 The Tibetan Plateau (~ 2,000,000 square kilometers) is the highest plateau in the
69 world with an average altitude of over 4000 meters above sea level. The Tibetan
70 Plateau is an ideal location for charactering rural and regional background aerosol due
71 to minor influences of anthropogenic activities. However, chemical characterization
72 of aerosol particles in the Tibetan Plateau is rather limited, and therefore their sources,
73 properties, and evolution processes are poorly known. Cong et al. (2015) reported the
74 seasonal variations of various aerosol components including carbonaceous species
75 and water-soluble ionic species on the south edge of the Tibetan Plateau. Sulfate was
76 found to dominate the total ionic mass (25%) followed by nitrate. In addition, most

77 aerosol species showed pronounced season variations in the pre-monsoon period due
78 to biomass burning impacts from India and Nepal. Zhao et al. (2013) also
79 characterized the chemical composition and sources of total suspended particulate
80 (TSP) at Lulang on the southeastern TP based on one year measurement. Similar
81 seasonal variations with higher concentrations during pre-monsoon were observed.
82 The back trajectory analysis showed evident transport of air pollutants from south
83 Asia to the TP. The analysis of size-segregated aerosol samples collected at a remote
84 site in the inland Tibetan Plateau during 2012 further confirmed the high
85 concentrations of organic carbon (OC) and elemental carbon (EC) during the
86 pre-monsoon period (Wan et al., 2015), although their concentrations in PM_{10} (2.38
87 and $0.08 \mu\text{g m}^{-3}$, respectively) were much lower than those reported in eastern China.
88 Most studies above were conducted in the southeastern Tibetan Plateau.
89 Comparatively, aerosol particles showed quite different behavior in the northeastern
90 Tibetan Plateau. Li et al. (2013) investigated the sources and chemical composition of
91 fine particles collected at a remote site (Qinghai Lake) in the summer of 2010 in the
92 Tibetan Plateau. The average $PM_{2.5}$ concentration was $22 \pm 13 \mu\text{g m}^{-3}$ with sulfate and
93 carbonaceous aerosol being the two major species. Xu et al. (2014b) conducted a
94 year-long measurement of $PM_{2.5}$ composition at the Qilian Shan Station, The annual
95 average concentration of $PM_{2.5}$ was $9.5 \pm 5.4 \mu\text{g m}^{-3}$ with water-soluble ions
96 accounting for 39% of total mass. Water-soluble ions were dominated by sulfate (39%)
97 and showed pronounced seasonal variations. The aerosol composition, size
98 distributions, and back trajectory analysis together indicated a mixed impact of both
99 mineral dust from arid areas of northwest China and anthropogenic emissions from
100 urban areas. However, previous extensive efforts to characterize the chemical
101 properties of aerosol particles in the Tibetan Plateau heavily rely on filter
102 measurements with the duration ranging from days to weeks, real-time measurement
103 of aerosol particle composition is still very limited. A recent study by Xu et al. (2014a)
104 deployed a high-resolution time-of-flight aerosol mass spectrometer (HR-ToF-AMS)
105 at an urban site in Lanzhou in northwest China. The submicron aerosol in the city was
106 dominated by organic aerosol (47%) with a large contribution from local traffic and

107 cooking emissions (40%). To our knowledge, there is no such real-time measurement
108 of aerosol particle composition with aerosol mass spectrometer at rural sites in the
109 Tibetan Plateau yet.

110 The study of new particle formation and growth events in the Tibetan Plateau is
111 also relatively new. Since 2004, a number of studies have been conducted to
112 investigate the new particle formation (NPF) and particle growth events in various
113 environments in China (Wu et al., 2007; Wiedensohler et al., 2009; Yue et al., 2010;
114 Zhang et al., 2011b; Wang et al., 2013a; Wang et al., 2013b). The NPF events were
115 frequently observed in urban cities, rural sites, coastal regions, and mountain sites.
116 Sulfuric acid was found to play a dominant role in both NPF and subsequent particle
117 growth, while organics makes an important contributor to particle growth (Yue et al.,
118 2010). The particle growth rates varied largely depending on sites and days, yet
119 generally fell within 1 – 20 nm hr⁻¹. Kivekas et al. (2009) conducted a long-term
120 measurement of particle number size distributions at Waliguan, a ~~global regional~~
121 ~~background site~~ ~~baseline site~~ located approximately 140 km southwest of our sampling
122 site. The annual average particle number concentration was found to be higher than
123 other rural sites in the world. Despite this, the particle growth and its relationship to
124 chemical species in the Tibetan Plateau are rarely investigated and remain poorly
125 understood.

126 In this study, an Aerodyne Aerosol Chemical Speciation Monitor (ACSM) was
127 first deployed at a national background monitoring site (Menyuan, Qinghai) in the
128 Tibetan Plateau for the real-time characterization of submicron aerosol composition
129 including organics, sulfate, nitrate, ammonium, and chloride from 5 September to 15
130 October, 2013. Collocated measurements including black carbon and particle number
131 size distributions were also conducted at the same site. Here we report the aerosol
132 composition and variations of submicron aerosols and investigate the sources of
133 organic aerosol with positive matrix factorization (PMF). In addition, the particle
134 growth events are also characterized and the roles of chemical species in particle
135 growth are elucidated.

136

137 2 Experimental method

138 2.1 Sampling site

139 The sampling site, i.e., the national atmospheric background monitoring station
140 (NBS) (37°36'30"N, 101°15'26"E, 3295 m a.s.l.) is located on the Daban Mountain in
141 Menyuan, Qinghai province (Fig. 1). The sampling site is characterized by a typical
142 Plateau continental climate with a pleasantly cool and short summer, and a long cold
143 winter. The annual average temperature is $-1\sim-2^{\circ}\text{C}$, and the precipitation is 426 - 860
144 mm. In this study, ambient temperature averaged 4.9°C ($-8.7 - 17.9^{\circ}\text{C}$) and wind
145 speed varied largely with an average value of 3 m s^{-1} . In addition, several precipitation
146 events were also observed, particularly during the first half period of this study (Fig.
147 3). The diurnal profiles of meteorological conditions including temperature, relative
148 humidity, wind speed, and wind direction are shown in Fig. S1. The sampling site is
149 relatively pristine with most areas covered by typical Tibetan Plateau plants, e.g.,
150 *potentilla fruticosa* and *kobresia* etc. –There are no strong local anthropogenic source
151 emissions in this area ($\sim 741\text{ km}^2$ with a population of ~ 2000) except occasional
152 biomass burning events **due to burning of a large amount of straws in the middle of**
153 **September and cow dung at the end of the campaign (Li et al., 2015). ~~that were~~**
154 **~~observed during this study.~~** The capital city Xining of Qinghai province with a
155 population of 2,290,000 is approximately 160 km south of the sampling site which is
156 connected by a national road G227 with few traffic vehicles.

157 2.2 Instrumentation

158 The field measurements were conducted from 5 September to 15 October 2013.
159 All the instruments were placed in an air-conditioned room with the temperature
160 maintaining at $\sim 23^{\circ}\text{C}$. The chemical compositions of non-refractory submicron
161 aerosol (NR-PM₁) species including organics (Org), sulfate (SO₄), nitrate (NO₃),
162 ammonium (NH₄) and chloride (Cl) were measured *in-situ* by an Aerodyne ACSM
163 (Ng et al., 2011b). A PM_{2.5} cyclone (Model: URG-2000-30ED) was supplied in front
164 of the sampling line to remove coarse particles larger than $2.5\text{ }\mu\text{m}$. The ambient air
165 was drawn inside the room through a 1/2 inch (outer diameter) stainless steel tube
166 using an external pump (flow rate is $\sim 3\text{ L min}^{-1}$). The sampling height is

167 approximately 2 m, and the particle residence time in the sampling tube is ~ 5s. A
168 silica gel diffusion dryer was then used to dry aerosol particles before sampling into
169 the ACSM. After passing through a 100 μm critical orifice, aerosol particles between
170 30 nm – 1 μm are focused into a narrow particle beam via the aerodynamic lens in the
171 vacuum chamber, and then flash vaporized and ionized at a heated surface (~600°C).
172 The positive ions generated are finally analyzed by a commercial quadrupole mass
173 spectrometer. In this study, the mass spectrometer of ACSM was operated at a
174 scanning rate of 500 ms amu^{-1} from m/z 10 to 150. The time resolution is
175 approximately 15 min by alternating 6 cycles between the ambient air and
176 particle-free air. The detailed operation of ACSM has been given in Sun et al.(2012).

177 In addition to ACSM measurements, a Scanning Mobility Particle Sizer (TSI,
178 3936) equipped with a long Differential Mobility Analyzer (DMA) was
179 simultaneously operated to measure the particle number size distributions between
180 11.8 nm – 478.3 nm at a time resolution of 5 min. Other collocated **species**
181 **measurements** included CO by a non-dispersive infrared analyser (M300EU), O₃ by a
182 UV photometric analyzer (Teledyne Instruments, Model 400EU), NO_x by a
183 commercial chemiluminescence analyzer (M200EU), and SO₂ by a pulsed UV
184 fluorescence analyzer (M100EU) ~~by various gas analyzers from Thermo Scientific~~
185 and black carbon (BC) by an Aethalometer (AE31, Magee Scientific Corp.). The
186 meteorological parameters, e.g., temperature, relative humidity, pressure, visibility,
187 precipitation, wind speed and wind direction were also recorded at the same site. All the
188 data are reported ~~with~~ at ambient conditions ~~at~~ in Beijing Standard Time. **Note that the**
189 **concentrations would be a factor of approximately 1.5 of the current values if the data**
190 **are converted to mass loadings at standard temperature and pressure (STP, 273K and**
191 **1013.25 hPa).**

192 **2.3 Data analysis**

193 The ACSM data were analyzed within Igor Pro (WaveMetrics, Inc., Oregon USA)
194 using the standard ACSM data analysis software (v.1.5.3.0). The mass concentrations
195 and chemical composition of NR-PM₁ species were obtained using the default relative
196 ionization efficiency (RIE) that is 1.4, 1.2, 1.1 and 1.3 for organics, sulfate, nitrate and

197 chloride, respectively, except ammonium (6.5) that was derived from pure ammonium
198 nitrate during ionization efficiency (IE) calibration. A collection efficiency (CE) of 0.5
199 was used to account for the incomplete detection of aerosol species (Matthew et al.,
200 2008; Middlebrook et al., 2012) because aerosol particles were dry and only slightly
201 acidic, and also the mass fraction of ammonium nitrate is not high enough to affect
202 CE significantly.

203 The sources of organic aerosol were investigated by performing Positive Matrix
204 Factorization (PMF2.exe, v 4.2) on ACSM OA mass spectra (Paatero and Tapper,
205 1994; Ulbrich et al., 2009). PMF is a standard multivariate factor analysis model
206 broadly used in the field of air pollution source apportionment. The detailed PMF
207 analysis of organic aerosol from AMS measurements, including error matrix
208 preparation, data pretreatment, selections of the optimum number of factors and
209 rotational forcing parameter (FPEAK), and the evaluation of PMF solutions was given
210 in Ulbrich et al. (2009) and Zhang et al. (2011a). In this study, the organic mass
211 spectra from m/z 12 to m/z 125 were used for the PMF analysis. Because of the
212 absence of collocated measurements, the two factor solution with $f_{\text{peak}} = 0$ and
213 Q/Q_{exp} close to 1 was chosen (see Fig. S2 for the PMF diagnostic plots). The two
214 factors including a biomass burning OA (BBOA) and an oxygenated OA (OOA) were
215 identified. The two OA factors showed largely different factor profiles and time series
216 indicating their distinct sources.

217 **3 Results and discussion**

218 **3.1 Mass concentration and chemical composition of submicron aerosol**

219 Figure 2 shows a comparison of the total PM_{10} mass (NR- PM_{10} + BC) with that
220 determined from the SMPS measurements. Assuming spherical particles, the SMPS
221 number concentrations were converted to the mass concentrations using
222 chemically-resolved particle density that was estimated from the chemical
223 composition of PM_{10} (Salcedo et al., 2006). As shown in Fig. 2, the time series of PM_{10}
224 tracks well with that of SMPS measurements ($r^2 = 0.87$). The slope of 0.52 is likely
225 due to the limited size range of SMPS measurements (12 – 478 nm) by missing a
226 considerable fraction of large particles that ACSM can measure. The PM_{10} mass varied

227 dramatically throughout the study with hourly average concentration ranging from 1.0
228 to 78.4 $\mu\text{g m}^{-3}$. The average mass concentration of PM_{10} ($\pm 1\sigma$) for the entire study is
229 11.4 (± 8.5) $\mu\text{g m}^{-3}$, which is $\sim 3 - 4$ times lower than those observed at rural sites in
230 China (29.9 – 44.1 $\mu\text{g m}^{-3}$) (Huang et al., 2011; Hu et al., 2013; Huang et al., 2013;
231 Zhang et al., 2014). It is also approximately twice lower than that (24.5 $\mu\text{g m}^{-3}$)
232 measured at an urban site in Lanzhou in the Tibetan Plateau in 2012 (Xu et al., 2014a).
233 While the average PM_{10} mass concentration in this study is close to those observed at
234 the remote sites in Asia, e.g., Okinawa (14.5 $\mu\text{g m}^{-3}$) (Zhang et al., 2007a) and Fukue
235 (12.0 $\mu\text{g m}^{-3}$) (Takami et al., 2005) in Japan in 2003, and Jeju (8.6 $\mu\text{g m}^{-3}$) in Korea in
236 2001 (Topping et al., 2004), it is much higher than those reported at rural/remote sites
237 in north America and Europe, e.g., Chebogue (2.9 $\mu\text{g m}^{-3}$), Storm Peak in 2004 (2.1
238 $\mu\text{g m}^{-3}$) and Hyytiälä in 2005 (2.0 $\mu\text{g m}^{-3}$), and even comparable to the loadings at
239 urban sites, e.g., New York City in 2004 (12 $\mu\text{g m}^{-3}$), Pittsburgh (15 $\mu\text{g m}^{-3}$), and
240 Manchester in 2002 (14.0 $\mu\text{g m}^{-3}$) (Zhang et al., 2007a). These results suggest that the
241 Menyuan NBS is a typical rural site in Asia, yet with higher background
242 concentrations compared to those in other continents.

243 Figure 3 shows the time series of mass concentrations and mass fractions of
244 aerosol species in PM_{10} . The average PM_{10} composition is dominated by organics and
245 sulfate on average accounting for 43% and 28%, respectively. Black carbon and
246 chloride represent small fractions contributing 4.5% and 1.2%, respectively to PM_{10} .
247 As shown in Fig. 1, the aerosol composition at the Menyuan NBS is largely different
248 from that observed at the urban site in the Tibetan Plateau (Xu et al., 2014a). In
249 particular, sulfate shows $\sim 60\%$ higher contribution, yet BC is more than twice lower
250 than that observed at the urban site (Fig. 1). Xu et al. (2014a) found that 47% of BC
251 was from local traffic emissions which well explained the higher contribution of BC
252 at the urban site. Compared to this study, the average composition of PM_{10} measured
253 by the AMS at other rural sites in China showed similar dominance of sulfate (25 –
254 34%) except Changdao Island (19%), yet overall higher contributions of nitrate
255 because most these rural sites are close to urban areas with high NO_x emissions. The
256 sulfate contributions become more dominant (36 – 64%) at remote sites in East Asia

257 which are far away from urban areas. The increase of sulfate contribution is
258 associated with a large reduction of nitrate contribution (< 5%). Such a change in
259 aerosol bulk composition at rural/remote sites in East Asia is shown Fig. 1. Overall,
260 organics comprises the major fraction of PM₁, contributing approximately one third of
261 the total mass at most sites. While sulfate plays a dominant role in PM₁ at remote sites,
262 nitrate shows the highest contribution at the rural sites in eastern China. Such
263 compositional differences illustrate the different sources of sulfate and nitrate. While
264 sulfate is dominantly from regional sources and transport, nitrate is more likely
265 influenced by anthropogenic NO_x emissions over a smaller regional areas.

266 Aerosol species also varied dramatically throughout the study. For example, the
267 organics increased rapidly from 2.9 μg m⁻³ to 77.8 μg m⁻³ in one hour on 21
268 September. While sulfate remained small variations, nitrate, chloride, and BC showed
269 similar steep increases as organics indicating strong impacts of local biomass burning
270 (Zhang et al., 2015). Rapid decreases of aerosol species due to the precipitation of
271 scavenging or wind direction change were also frequently observed. For a better
272 understanding aerosol composition under variable meteorological conditions and
273 sources, five episodes with two of them from clean periods are shown in Fig. 3d. The
274 aerosol composition varied largely among different episodes. While the average PM₁
275 mass concentrations during the two clean episodes are similar (3.6 and 3.8 μg m⁻³),
276 the episode of Clean2 shows much higher contribution of organics (48% vs. 34%)
277 with slightly lower sulfate (33% vs. 36%) than Clean 1, consistent with their different
278 air mass trajectories (Fig. S3). The other three episodes show ~5 – 8 times higher
279 mass concentration of PM₁ (17.6 – 27.2 μg m⁻³) than the two clean episodes. The Ep1
280 is dominated by organics (70%), almost twice of those during the other two episodes
281 suggesting a largely different source. The relative contributions of sulfate and
282 organics during Ep2 and Ep3 are different although the nitrate contribution is similar.
283 These results suggest that the national background site is subject to the influences of
284 air masses from different sources, some of which are enriched with OA while others
285 are dominated with aerosols mainly composed of ammonium sulfates. We also
286 noticed that the two clean periods showed overall higher contribution of sulfate and

287 lower contribution of nitrate compared to the three pollution episodes. The possible
288 reasons were likely due to that the air masses during clean periods were either from a
289 longer transport when ammonium nitrate was deposited or evaporated due to dilution
290 processes, or from less anthropogenic influenced regions with low NO_x emissions.

291 The aerosol particle acidity was evaluated using the ratio of measured NH₄⁺
292 (NH₄⁺_{meas}) to the predicted NH₄⁺ (NH₄⁺_{pred} = 18×(2×SO₄²⁻/96+NO₃⁻/62+Cl⁻/35.5) that
293 needs to fully neutralize sulfate, nitrate, and chloride (Zhang et al., 2007b). The
294 NH₄⁺_{meas} correlates tightly with NH₄⁺_{pred} (r² = 0.95), yielding a regression slope of
295 0.80. The results suggest that aerosol particles at the **Menyuan** NBS are overall acidic.
296 Similar acidic particles were also observed at other rural sites in China, e.g., Jiaxing in
297 Yangtze River Delta (Huang et al., 2013), Kaiping in Pearl River Delta (Huang et al.,
298 2011), Yufa in Beijing (Takegawa et al., 2009), and Qilianshan Mountain in the
299 northeast of the Qinghai–Xizang Plateau (Xu et al., 2015). As a comparison, the
300 aerosol particles in the urban city Lanzhou in the Tibetan Plateau were overall
301 neutralized (Xu et al., 2014a). One of the explanations is that more SO₂ is oxidized to
302 sulfate during the transport while gaseous ammonia is not enough to neutralize the
303 newly formed sulfate. This is supported by the overall higher contribution of sulfate at
304 rural/remote sites than that at urban sites. Also note that the newly formed sulfate
305 particles during the frequent NPF events might also have played a role.

306 **3.2 Diurnal variations**

307 The diurnal cycles of aerosol species and PM₁ are shown in Fig. 4a. The PM₁
308 shows a pronounced diurnal cycle with the concentration ranging from 7.9 to 13.4 μg
309 m⁻³. The PM₁ shows a visible peak at noon time and then has a gradual decrease
310 reaching the minimum approximately at 16:00. After that, the PM₁ starts to build up
311 and reaches the highest level at midnight. Such a diurnal cycle is similar to those of
312 SO₂ and CO (Fig. 4d), which likely indicates that the major source of PM₁ at the
313 **Menyuan** NBS is from regional transport. All aerosol species present similarly
314 pronounced diurnal cycles to PM₁ with the lowest concentrations occurring
315 approximately at 16:00, indicating that the diurnal cycles of aerosol species were
316 mainly driven by the dynamics of planetary boundary layer. Organics dominated PM₁

317 composition throughout the day varying from 38% - 51%. The concentration of
318 organics at 16:00 is approximately twice lower than that at midnight. Sulfate shows
319 the largest noon peak among all aerosol species, consistent with those of SO₂ and CO.
320 The sulfate contributes more than 25% to PM₁ with the highest contribution as much
321 as 33% between 12:00 – 14:00. Nitrate and chloride shows relatively stable
322 concentrations before 11:00 and then gradually decreased to low ambient levels
323 during daytime. Such diurnal variations still exist after considering the dilution effects
324 of boundary layer height using the conserved tracer CO as a reference (Fig. 4c). This
325 indicates that gas-particle partitioning affected by temperature and humidity has
326 played an important role in driving the diurnal variations of nitrate and chloride.
327 Consistently, the nitrate contribution to PM₁ during late afternoon is ~7-8% which is
328 much lower than that (> 12%) in the early morning. The diurnal variation of BC is
329 different from that observed at the urban site in the Tibetan Plateau where the
330 pronounced morning peak due traffic influences was observed (Xu et al., 2014a). In
331 fact, BC has a good correlation with secondary nitrate ($r^2 = 0.59$) indicating that BC is
332 likely dominantly from regional transport. This is also supported by the low ambient
333 levels of NO_x (2.5 – 5.1 μg m⁻³). The contribution of BC to PM₁ is relatively constant,
334 which is ~ 4 – 5% throughout the day.

335 **3.3 OA composition and sources**

336 PMF analysis of ACSM OA mass spectra identified two factors, i.e., a biomass
337 burning OA (BBOA) and an oxygenated OA (OOA). The mass spectra and time
338 series of the two OA factors are shown in Fig. 5.

339 **3.3.1 BBOA**

340 The mass spectrum of BBOA resembles to that of standard BBOA ($r^2 = 0.82$)
341 which is characterized by a prominent peak of m/z 60 (1.1% of total signal), a tracer
342 m/z for biomass burning aerosols (Aiken et al., 2009; Cubison et al., 2011; Hennigan
343 et al., 2011). The fraction of m/z 60 in BBOA (1.1%) is also much higher than ~0.3%
344 in the absence of biomass burning impacts (Cubison et al., 2011). BBOA correlates
345 tightly with m/z 60 ($r^2 = 0.82$) and also chloride ($r^2 = 0.52$). The ratio of BBOA to m/z
346 60 is 55.6, which is higher than that of fresh BBOA (34.5) measured during the

347 second Fire Lab at Missoula Experiment (FLAME II) (Lee et al., 2010). One of the
348 explanations is that BBOA in the ambient is more aged because the m/z 60 related
349 levoglucosan can be rapidly oxidized in the atmosphere (Hennigan et al., 2010).
350 Indeed, Zhang et al. (2015) reported a much higher ratio of aged BBOA to m/z 60
351 (74.8) than fresh BBOA (16.8) during two harvest seasons in Nanjing, China. The
352 time series of BBOA shows periodically large peaks, particularly on the days of 21
353 and 22 September, which were mainly from the burning of a large amount of straws in
354 the south-west region. Relatively high concentration of BBOA was also observed at
355 the end of the campaign due to the burning of cow dung for heating purpose because
356 of the low temperature. The average concentration of BBOA is $0.8 (\pm 1.5) \mu\text{g m}^{-3}$ for
357 the entire study on average accounting for 15% of total OA. Although the average
358 BBOA contribution is much lower than those measured in PRD, e.g., Jiaxing ($\sim 3.9 \mu\text{g m}^{-3}$,
359 30.1%) (Huang et al., 2013), Kaiping ($\sim 1.36 \mu\text{g m}^{-3}$, 24.5%) (Huang et al., 2011),
360 and Shenzhen ($\sim 5.2 \mu\text{g m}^{-3}$, 29.5%) (He et al., 2011), the contribution of BBOA
361 during some strong BB plumes can reach up to 40%, e.g., 21-22 September,
362 indicating a large impact of biomass burning on OA at the national background site.
363 BBOA showed a pronounced diurnal cycle which is similar to that of chloride (Fig.
364 5c). The BBOA concentration increased rapidly from 18:00 and reached a maximum
365 in 2 hours, likely indicating that the burning of straws and cow dung mainly occurred
366 during this period of time. As a result, the contribution of BBOA to total OA increased
367 from $\sim 10\%$ to more than 20%.

368 **3.3.2 Oxygenated organic aerosols (OOA)**

369 Similar to previously reported OOA (Zhang et al., 2005), the mass spectrum of
370 OOA in this study is characterized by a prominent m/z 44 peak (mainly CO_2^+). The
371 mass spectrum of OOA also resembles to that of low-volatility OOA ($r^2 = 0.88$) (Ng
372 et al., 2011a), yet with higher fraction of m/z 44 (f_{44}). Much higher fraction of m/z 44
373 in ACSM OOA spectrum than that from HR-ToF-AMS was reported recently by a
374 comprehensive evaluation of the ACSM (Fröhlich et al., 2015). The results also
375 showed that f_{44} has minor impacts on the mass concentrations of OOA factors,
376 although it varies largely by a factor of 0.6 – 1.3. The average mass concentration of

377 OOA is $4.1 \mu\text{g m}^{-3}$, on average accounting for 85% of total OA. The OOA
378 contribution is much higher than those reported at urban sites in summer (~60%)
379 (Huang et al., 2010; Sun et al., 2012; Xu et al., 2014a), and also higher than those
380 (~70%) observed at rural sites in China (Hu et al., 2013; Huang et al., 2013). These
381 results suggest that organic aerosol was highly aged and well processed at the
382 | **Menyuan** NBS. In addition, aqueous-processing of OA at nighttime associated with
383 high RH might also played a role in forming the highly oxidized OA. The diurnal
384 cycle of OOA was similar to that of PM_{10} , which showed a small peak before noon
385 time followed by a subsequent decrease until 16:00. The OOA dominated OA
386 | throughout the day varying from 80 – 90%, indicating that OA at the **Menyuan** NBS
387 was mainly composed of secondary organic aerosol.

388 Previous studies have shown the ubiquitously tight correlations between sulfate
389 and highly oxidized OA because of their similar secondary nature over regional scales
390 (Zhang et al., 2005; DeCarlo et al., 2010). While the OOA correlates well with
391 secondary sulfate for most of the time in this study, several periods with largely
392 | different correlations were also observed (Fig. 6). As shown in Figs. 5b and 6, the
393 weak correlation events mainly occurred during periods with strong biomass burning
394 impacts were observed. However, it cannot be resolved by extending PMF solution to
395 more than 2 factors because of the limitation of PMF technique in source
396 apportionment analysis. Similar different correlations between sulfate and LV-OOA
397 were also observed during two research flights in Mexico City and the Central
398 Mexican Plateau (DeCarlo et al., 2010). Following the approach suggested by
399 DeCarlo et al. (2010), we performed a post-processing technique with external tracers
400 on the further apportionment of OOA. We first assume that OOA and sulfate have
401 similar sources during periods in the absence of biomass burning impacts, which is
402 supported by their tight correlations ($r^2 = 0.74$). An average OOA/ SO_4 ratio of 1.04,
403 i.e., $(\text{OOA}/\text{SO}_4)_{\text{NBB}}$, was obtained by performing a linear regression analysis on OOA
404 versus SO_4 . We then assume that SO_4 is completely from non-biomass burning (NBB)
405 sources during BB-impact periods. This assumption is rational because previous
406 studies have found that fresh biomass burning emits a very small or negligible

407 fraction of sulfate (Levin et al., 2010). The sulfate-related OOA can be calculated as
408 $OOA \times [OOA/SO_4]_{NBB}$, and the excess OOA that is from different sources is then
409 determined as:

$$410 \quad OOA_{\text{post-processed}} = OOA - SO_4 \times [OOA/SO_4]_{NBB} \quad (1)$$

411 Because the post-processed OOA shows high concentrations during BB periods, we
412 conclude that it's very likely an aged BBOA that was mixed with OOA. In fact, the
413 mass spectrum of $OOA_{\text{post-processed}}$ is similar to that of OOA. The fraction of m/z 60 (f_{60})
414 is 0.29%, which is very close to $\sim 0.3\%$ for non-biomass burning organic aerosol
415 (Aiken et al., 2008). Smog chamber experiments have shown that fresh BBOA can be
416 rapidly oxidized within 3 – 4.5 hours (Hennigan et al., 2011). While f_{44} increases
417 significantly, f_{60} quickly decreases to a value close to $\sim 0.3\%$. Similarly, a recent study
418 in Nanjing resolved an aged BBOA factor with its spectrum resembling to that of
419 OOA yet with much lower f_{60} (Zhang et al., 2015). The average concentration of aged
420 BBOA is $0.82 (\pm 2.65) \mu\text{g m}^{-3}$, accounting for 17% of OA for the entire study. The
421 contribution of aged BBOA is close to that of fresh BBOA, which might indicate that
422 half of BBOA has been aged. Still, the sum of fresh and aged BBOA highly correlates
423 with m/z 60 ($r^2 = 0.81$, slope = 136.1). The fresh and aged BBOA together accounted
424 for 33% of the total OA suggesting that BBOA was a large local source of OA during
425 the observational period. With the post-processing technique, the sulfate-related OOA
426 contributed 67% on average of total OA, which is close to those observed at other
427 rural sites in e.g., Kaiping (Huang et al., 2011) and Changdao (Hu et al., 2013).

428 **3.4 Chemistry of particle growth**

429 Figure 7a shows the evolution of size distributions of particle number
430 concentrations for the entire study. New particle formation and growth events (NPE)
431 were observed almost every day (27 days in 34 days). Most NPE started at $\sim 11:00$
432 (The time of sunrise is 2 hours behind of Beijing standard time) and persisted more
433 than half day except some NPE were interrupted by either precipitation events or
434 strong winds. The average particle number size distributions during NPE and non
435 event days (non-NPE) are shown in Fig. 7b. Both NPE and non-NPE show broad size
436 distributions with higher number concentrations occurring during NPE. Three modes

437 with geometric mean diameter (GMD) peaking at 28 nm, 43 nm, and 104 nm,
438 respectively were resolved using a log-normal distribution fitting (Seinfeld and Pandis,
439 2006). The largest mode (104 nm) dominated the total number of particles accounting
440 for ~70%. In contrast, the average size distribution during non-NPE was characterized
441 by a bi-modal distribution with the GMD peaking at 59 nm and 146 nm, respectively.
442 The peak diameters were shifted to the larger sizes compared to those during NPE.
443 Such a size shift from clean days to polluted days was also observed previously in
444 Beijing (Yue et al., 2010). Also, the two modes showed almost equivalent
445 contributions to the total number of particles. The average particle number
446 concentration for the entire study is $2.4 \times 10^3 \text{ cm}^{-3}$, which is nearly an order of
447 magnitude lower than those reported at rural sites in eastern China (Wu et al., 2007),
448 but close to that ($2.03 \times 10^3 \text{ cm}^{-3}$) observed at Mount Waliguan which is a remote site
449 located nearby (Kivekas et al., 2009). The particle size was further segregated into
450 small Aitken mode (20 – 40 nm, N_{20-40}), large Aitken mode (40 – 100 nm, N_{40-100}),
451 and Accumulation mode (100 – 470 nm, N_{Accu}) particles. The time series and diurnal
452 cycles of particle numbers for three different sizes are shown in Fig. 7c, d. The N_{20-40}
453 presented sharp peaks almost in everyday corresponding to new particle formation
454 events. The diurnal cycle of N_{20-40} showed that the number concentration started to
455 increase at approximately 11:00 (150 cm^{-3}) and reached a maximum at 14:00 (770
456 cm^{-3}). In contrast, the N_{40-100} and N_{Accu} showed largely different diurnal cycles from
457 that of N_{20-40} , indicating their different sources. In fact, the diurnal cycles of N_{40-100}
458 and N_{Accu} are remarkably similar to those of aerosol species, suggesting that the large
459 particles are more likely from regional transport.

460 Figure 8 shows the diurnal evolution of particle number size distributions, aerosol
461 composition, and gaseous species during NPE and non-NPE days. The particle
462 number size distributions during NPE were characterized by distinct bimodal
463 distributions showing a persistent larger mode with the GMD peaking at ~100 nm,
464 and a smaller mode below 50 nm. The particle growth started at approximately 11:00
465 from ~20 nm, and continued to grow slowly until ~45 nm at mid-night. The maximum
466 size particles can grow in this study is generally smaller than those (~60 – 70 nm)

467 observed at urban and rural sites in Beijing (Wang et al., 2013a), which is likely due
468 to the much lower concentrations of aerosol species and precursors. All aerosol
469 species however showed decreases during the particle growth period between 12:00 –
470 17:00, and the gaseous CO and SO₂ showed similar variations as aerosol species. By
471 excluding the dilution effect of PBL using CO as a tracer, we found that organics was
472 the only species showing a gradual increase during the particle growth period (Fig. 8a)
473 while other species remained minor changes or even slightly decreased. The
474 contribution of organics to PM₁ also showed a corresponding increase from 40% to
475 47%. These results suggest that organics might have played a dominant role in
476 particle growth at the national background site. Our conclusion is consistent with the
477 recent findings that organics, particularly oxidized organic aerosol species, play a
478 more important role than ammonium sulfate in particle growth (Dusek et al., 2010;
479 Ehn et al., 2014; Setyan et al., 2014). Also note that the contribution of organics to
480 PM₁ during NPE (~40 – 50%) is overall higher than that during non-NPE (~30 –
481 40%), while the sulfate contribution is correspondingly lower (~20 – 30% vs. 30 –
482 40%), which further supports the important role of organics during NPE. The particle
483 growth was mixed with anthropogenic sources from 17:00 which are indicated by
484 synchronous enhancements of both aerosol species and gaseous precursors. One of
485 possible reasons is due to the air mass transport from downwind urban areas.

486 The diurnal evolution of particle size distributions and aerosol composition
487 during non-NPE is largely different from that during NPE. The particle number size
488 distributions and mass concentrations of aerosol species showed a dramatic variation
489 at noon time (12:00), indicating a very different chemical and/or physical process
490 between the first and the second half day. The aerosol particles showed an evident
491 growth from ~50 nm to 60 nm during the first 6 hours, which is likely a continuation
492 of previous NPE. Compared to the early stage of particle growth during NPE, the
493 particle growth during non-NPE is associated with synchronous increases of both
494 organics and sulfate. The results indicate that both organics and sulfate contribute to
495 the particle growth after mixed with anthropogenic sources from ~18:00 in the
496 previous day.

497 We further calculated the particle growth rates (GR) for NPE events without
498 interruptions due to meteorological changes using Eq. (2).

$$499 \quad \text{GR} = \frac{\Delta D_m}{\Delta t} \quad (2)$$

500 | **W**here D_m is the geometric mean diameter from the log-normal fitting, ΔD_m is the
501 difference of diameter during the growth period and Δt is the duration of growth time.
502 The calculated GR and the corresponding average chemical composition and fraction
503 of OOA during the growth period are shown in Fig. 9a. The GR ranges from 0.8 nm
504 h^{-1} to 3.2 nm h^{-1} with an average of 2.0 nm h^{-1} . The GR in this study is overall
505 consistent with those observed at remote and/or forest sites (Eisele and McMurry,
506 1997; Weber et al., 1997), yet generally smaller than those measured at urban and
507 polluted rural sites (Yue et al., 2010; Shen et al., 2011; Zhang et al., 2011b) where
508 abundant condensable vapor and high concentrations of particulate matter facilitate
509 the growth of particles (Wang et al., 2013a). By linking GR to aerosol composition,
510 we found that GR at the background site is positively related to the fraction of
511 oxidized OA, which likely indicate the important role of oxidized secondary organic
512 aerosol in particle growth (Ehn et al., 2014). Zhang et al. (2011b) also observed a
513 tight correlation between OOA and GR in urban Beijing supporting the important role
514 of OOA in particle growth. Further investigation is needed for a better understanding
515 of the role of organic aerosol, particularly oxidized OA, in the new particle formation
516 and particle growth at the regional background site.

517 **4 Conclusions**

518 The aerosol particle composition and particle number size distributions were
519 measured at a national background monitoring station in the Tibetan Plateau (3295 m,
520 a.s.l.) from 5 September to 15 October 2013. The average mass concentration of PM_{10}
521 is 11.4 (\pm 8.5) $\mu\text{g m}^{-3}$ for the entire study, which is lower than those observed at urban
522 and rural sites in eastern China. Organics constituted the major fraction of PM_{10} , on
523 average accounting for 43% followed by sulfate (28%) and ammonium (11%).
524 Several periods with the contribution of organics as much as 70% due to biomass
525 burning impacts were also observed. All aerosol species presented similar diurnal

526 cycles that were mainly driven by the dynamics of planetary boundary layer and
527 regional transport. PMF source apportionment analysis resolved a secondary OOA
528 and a primary BBOA. OOA dominated OA composition accounting for 85% on
529 average with the rest being BBOA. A post-processing technique based on the
530 correlation of OOA and sulfate separated an aged BBOA which on average accounted
531 for 17% of OA. New particle formation and particle growth events were frequently
532 observed during this study. The particle growth rates varied from 0.8 to 3.2 nm hr⁻¹
533 with an average growth rate of 2.0 nm hr⁻¹. Organics was found to be the only species
534 with gradually increased contribution to PM₁ during NPE. Also, higher contribution
535 of organics during NPE than non-NPE days was observed. These results potentially
536 illustrate the important role of organics in particle growth. Further analysis showed a
537 positive correlation of particle growth rate with the fraction of OOA suggesting that
538 oxidized OA plays a critical role contributing to the particle growth.

539

540 **Acknowledgements**

541 This work was supported by the National Natural Science Foundation of China
542 (41375133), the National Key Project of Basic Research (2013CB955801), and the
543 Strategic Priority Research Program (B) of the Chinese Academy of Sciences (Grant
544 No. XDB050205001). We thank the National Station for Background Atmospheric
545 Monitoring for providing the meteorological data and gaseous data.

546

547

548 **References**

- 549 Aiken, A. C., DeCarlo, P. F., Kroll, J. H., Worsnop, D. R., Huffman, J. A., Docherty, K. S., Ulbrich, I.
550 M., Mohr, C., Kimmel, J. R., Sueper, D., Sun, Y., Zhang, Q., Trimborn, A., Northway, M.,
551 Ziemann, P. J., Canagaratna, M. R., Onasch, T. B., Alfarra, M. R., Prevot, A. S. H., Dommen,
552 J., Duplissy, J., Metzger, A., Baltensperger, U., and Jimenez, J. L.: O/C and OM/OC ratios of
553 primary, secondary, and ambient organic aerosols with High-Resolution Time-of-Flight
554 Aerosol Mass Spectrometry, *Environ. Sci. Technol.*, 42, 4478-4485, 2008.
- 555 Aiken, A. C., Salcedo, D., Cubison, M. J., Huffman, J. A., DeCarlo, P. F., Ulbrich, I. M., Docherty,
556 K. S., Sueper, D., Kimmel, J. R., Worsnop, D. R., Trimborn, A., Northway, M., Stone, E. A.,
557 Schauer, J. J., Volkamer, R. M., Fortner, E., de Foy, B., Wang, J., Laskin, A., Shutthanandan,
558 V., Zheng, J., Zhang, R., Gaffney, J., Marley, N. A., Paredes-Miranda, G., Arnott, W. P.,

559 Molina, L. T., Sosa, G., and Jimenez, J. L.: Mexico City aerosol analysis during MILAGRO
560 using high resolution aerosol mass spectrometry at the urban supersite (T0) - Part 1: Fine
561 particle composition and organic source apportionment, *Atmos. Chem. Phys.*, 9,
562 6633-6653, 2009.

563 Cao, J., Lee, S., Chow, J. C., Watson, J. G., Ho, K., Zhang, R., Jin, Z., Shen, Z., Chen, G., and Kang,
564 Y.: Spatial and seasonal distributions of carbonaceous aerosols over China, *J. Geophys.*
565 *Res.*, 112, 2007.

566 Cong, Z., Kang, S., Kawamura, K., Liu, B., Wan, X., Wang, Z., Gao, S., and Fu, P.: Carbonaceous
567 aerosols on the south edge of the Tibetan Plateau: concentrations, seasonality and
568 sources, *Atmos. Chem. Phys.*, 15, 1573-1584, 10.5194/acp-15-1573-2015, 2015.

569 Cubison, M. J., Ortega, A. M., Hayes, P. L., Farmer, D. K., Day, D., Lechner, M. J., Brune, W. H.,
570 Apel, E., Diskin, G. S., Fisher, J. A., Fuelberg, H. E., Hecobian, A., Knapp, D. J., Mikoviny, T.,
571 Riemer, D., Sachse, G. W., Sessions, W., Weber, R. J., Weinheimer, A. J., Wisthaler, A., and
572 Jimenez, J. L.: Effects of aging on organic aerosol from open biomass burning smoke in
573 aircraft and laboratory studies, *Atmos. Chem. Phys.*, 11, 12049-12064,
574 10.5194/acp-11-12049-2011, 2011.

575 DeCarlo, P. F., Ulbrich, I. M., Crouse, J., de Foy, B., Dunlea, E. J., Aiken, A. C., Knapp, D.,
576 Weinheimer, A. J., Campos, T., Wennberg, P. O., and Jimenez, J. L.: Investigation of the
577 sources and processing of organic aerosol over the Central Mexican Plateau from aircraft
578 measurements during MILAGRO, *Atmos. Chem. Phys.*, 10, 5257-5280,
579 10.5194/acp-10-5257-2010, 2010.

580 Dusek, U., Frank, G. P., Curtius, J., Drewnick, F., Schneider, J., Kürten, A., Rose, D., Andreae, M.
581 O., Borrmann, S., and Pöschl, U.: Enhanced organic mass fraction and decreased
582 hygroscopicity of cloud condensation nuclei (CCN) during new particle formation events,
583 *Geophys. Res. Lett.*, 37, L03804, 10.1029/2009gl040930, 2010.

584 Ehn, M., Thornton, J. A., Kleist, E., Sipila, M., Junninen, H., Pullinen, I., Springer, M., Rubach,
585 F., Tillmann, R., Lee, B., Lopez-Hilfiker, F., Andres, S., Acir, I.-H., Rissanen, M., Jokinen, T.,
586 Schobesberger, S., Kangasluoma, J., Kontkanen, J., Nieminen, T., Kurten, T., Nielsen, L. B.,
587 Jorgensen, S., Kjaergaard, H. G., Canagaratna, M., Maso, M. D., Berndt, T., Petaja, T.,
588 Wahner, A., Kerminen, V.-M., Kulmala, M., Worsnop, D. R., Wildt, J., and Mentel, T. F.: A
589 large source of low-volatility secondary organic aerosol, *Nature*, 506, 476-479,
590 10.1038/nature13032, 2014.

591 Eisele, F. L., and McMurry, P. H.: Recent progress in understanding particle nucleation and
592 growth, *Philosophical Transactions of the Royal Society B: Biological Sciences*, 352,
593 191-201, 10.1098/rstb.1997.0014, 1997.

594 Fröhlich, R., Crenn, V., Setyan, A., Belis, C. A., Canonaco, F., Favez, O., Riffault, V., Slowik, J. G.,
595 Aas, W., Aijälä, M., Alastuey, A., Artiñano, B., Bonnaire, N., Bozzetti, C., Bressi, M.,
596 Carbone, C., Coz, E., Croteau, P. L., Cubison, M. J., Esser-Gietl, J. K., Green, D. C., Gros, V.,
597 Heikkinen, L., Herrmann, H., Jayne, J. T., Lunder, C. R., Minguillón, M. C., Močnik, G.,
598 O'Dowd, C. D., Ovadnevaite, J., Petralia, E., Poulain, L., Priestman, M., Ripoll, A.,
599 Sarda-Estève, R., Wiedensohler, A., Baltensperger, U., Sciare, J., and Prévôt, A. S. H.:
600 ACTRIS ACSM intercomparison – Part 2: Intercomparison of ME-2 organic source
601 apportionment results from 15 individual, co-located aerosol mass spectrometers, *Atmos.*
602 *Meas. Tech. Discuss.*, 8, 1559-1613, 10.5194/amtd-8-1559-2015, 2015.

603 Gong, Z., Lan, Z., Xue, L., Zeng, L., He, L., and Huang, X.: Characterization of submicron
604 aerosols in the urban outflow of the central Pearl River Delta region of China, *Front.*
605 *Environ. Sci. Eng.*, 10.1007/s11783-012-0441-8, 2012.

606 He, L.-Y., Huang, X.-F., Xue, L., Hu, M., Lin, Y., Zheng, J., Zhang, R., and Zhang, Y.-H.: Submicron
607 aerosol analysis and organic source apportionment in an urban atmosphere in Pearl
608 River Delta of China using high-resolution aerosol mass spectrometry, *J. Geophys. Res.*,
609 116, 10.1029/2010jd014566, 2011.

610 Hennigan, C. J., Sullivan, A. P., Collett, J. L., and Robinson, A. L.: Levoglucosan stability in
611 biomass burning particles exposed to hydroxyl radicals, *Geophys. Res. Lett.*, 37, L09806,
612 doi:10.1029/2010GL043088, 2010.

613 Hennigan, C. J., Miracolo, M. A., Engelhart, G. J., May, A. A., Presto, A. A., Lee, T., Sullivan, A.
614 P., McMeeking, G. R., Coe, H., Wold, C. E., Hao, W. M., Gilman, J. B., Kuster, W. C., de
615 Gouw, J., Schichtel, B. A., Collett, J. L., Kreidenweis, S. M., and Robinson, A. L.: Chemical
616 and physical transformations of organic aerosol from the photo-oxidation of open
617 biomass burning emissions in an environmental chamber, *Atmos. Chem. Phys.*, 11,
618 7669-7686, 10.5194/acp-11-7669-2011, 2011.

619 Hu, W. W., Hu, M., Yuan, B., Jimenez, J. L., Tang, Q., Peng, J. F., Hu, W., Shao, M., Wang, M.,
620 Zeng, L. M., Wu, Y. S., Gong, Z. H., Huang, X. F., and He, L. Y.: Insights on organic aerosol
621 aging and the influence of coal combustion at a regional receptor site of central eastern
622 China, *Atmos. Chem. Phys.*, 13, 10095-10112, 10.5194/acp-13-10095-2013, 2013.

623 Huang, X.-F., Xue, L., Tian, X.-D., Shao, W.-W., Sun, T.-L., Gong, Z.-H., Ju, W.-W., Jiang, B., Hu,
624 M., and He, L.-Y.: Highly time-resolved carbonaceous aerosol characterization in Yangtze
625 River Delta of China: composition, mixing state and secondary formation, *Atmos.*
626 *Environ.*, 64, 200 - 207, 10.1016/j.atmosenv.2012.09.059, 2013.

627 Huang, X. F., He, L. Y., Hu, M., Canagaratna, M. R., Sun, Y., Zhang, Q., Zhu, T., Xue, L., Zeng, L.
628 W., Liu, X. G., Zhang, Y. H., Jayne, J. T., Ng, N. L., and Worsnop, D. R.: Highly time-resolved
629 chemical characterization of atmospheric submicron particles during 2008 Beijing
630 Olympic Games using an Aerodyne High-Resolution Aerosol Mass Spectrometer, *Atmos.*
631 *Chem. Phys.*, 10, 8933-8945, 10.5194/acp-10-8933-2010, 2010.

632 Huang, X. F., He, L. Y., Hu, M., Canagaratna, M. R., Kroll, J. H., Ng, N. L., Zhang, Y. H., Lin, Y.,
633 Xue, L., Sun, T. L., Liu, X. G., Shao, M., Jayne, J. T., and Worsnop, D. R.: Characterization of
634 submicron aerosols at a rural site in Pearl River Delta of China using an Aerodyne
635 High-Resolution Aerosol Mass Spectrometer, *Atmos. Chem. Phys.*, 11, 1865-1877,
636 10.5194/acp-11-1865-2011, 2011.

637 Huang, X. F., He, L. Y., Xue, L., Sun, T. L., Zeng, L. W., Gong, Z. H., Hu, M., and Zhu, T.: Highly
638 time-resolved chemical characterization of atmospheric fine particles during 2010
639 Shanghai World Expo, *Atmos. Chem. Phys.*, 12, 4897-4907, 10.5194/acp-12-4897-2012,
640 2012.

641 Jacobson, M. Z.: Strong radiative heating due to the mixing state of black carbon in
642 atmospheric aerosols, *Nature*, 409, 695-697,
643 http://www.nature.com/nature/journal/v409/n6821/supinfo/409695a0_S1.html, 2001.

644 Jiang, Q., Sun, Y. L., Wang, Z., and Yin, Y.: Aerosol composition and sources during the
645 Chinese Spring Festival: fireworks, secondary aerosol, and holiday effects, *Atmos.*
646 *Chem. Phys.*, 15, 6023-6034, 10.5194/acp-15-6023-2015, 2015.

647 Kivekas, N., Sun, J., Zhan, M., Kerminen, V. M., Hyvärinen, A., Komppula, M., Viisanen, Y.,
648 Hong, N., Zhang, Y., Kulmala, M., Zhang, X. C., Deli, G., and Lihavainen, H.: Long term
649 particle size distribution measurements at Mount Waliguan, a high-altitude site in inland
650 China, *Atmos. Chem. Phys.*, 9, 5461-5474, 2009.

651 Lee, T., Sullivan, A. P., Mack, L., Jimenez, J. L., Kreidenweis, S. M., Onasch, T. B., Worsnop, D.
652 R., Malm, W., Wold, C. E., Hao, W. M., and Collett, J. L.: Chemical Smoke Marker
653 Emissions During Flaming and Smoldering Phases of Laboratory Open Burning of
654 Wildland Fuels, *Aerosol Sci. Technol.*, 44, i-v, 10.1080/02786826.2010.499884, 2010.

655 Levin, E. J. T., McMeeking, G. R., Carrico, C. M., Mack, L. E., Kreidenweis, S. M., Wold, C. E.,
656 Moosmüller, H., Arnott, W. P., Hao, W. M., Collett, J. L., Jr., and Malm, W. C.: Biomass
657 burning smoke aerosol properties measured during Fire Laboratory at Missoula
658 Experiments (FLAME), *J. Geophys. Res.*, 115, D18210, 10.1029/2009jd013601, 2010.

659 Li, J. J., Wang, G. H., Wang, X. M., Cao, J. J., Sun, T., Cheng, C. L., Meng, J. J., Hu, T. F., and Liu,
660 S. X.: Abundance, composition and source of atmospheric PM 2.5 at a remote site in the
661 Tibetan Plateau, China, *Tellus B*, 65, 2013.

662 Li, W. J., Chen, S. R., Xu, Y. S., Guo, X. C., Sun, Y. L., Yang, X. Y., Wang, Z. F., Zhao, X. D., Chen, J.
663 M., and Wang, W. X.: Mixing state, composition, and sources of fine aerosol particles in the
664 Qinghai-Tibetan Plateau and the influence of agricultural biomass burning, *Atmos. Chem.
665 Phys. Discuss.*, 15, 24369-24401, 10.5194/acpd-15-24369-2015, 2015.

666 Matthew, B. M., Middlebrook, A. M., and Onasch, T. B.: Collection efficiencies in an Aerodyne
667 Aerosol Mass Spectrometer as a function of particle phase for laboratory generated
668 aerosols, *Aerosol Sci. Technol.*, 42, 884-898, 10.1080/02786820802356797, 2008.

669 Middlebrook, A. M., Bahreini, R., Jimenez, J. L., and Canagaratna, M. R.: Evaluation of
670 Composition-Dependent Collection Efficiencies for the Aerodyne Aerosol Mass
671 Spectrometer using Field Data, *Aerosol Sci. Technol.*, 46, 258-271,
672 10.1080/02786826.2011.620041, 2012.

673 Ng, N. L., Canagaratna, M. R., Jimenez, J. L., Zhang, Q., Ulbrich, I. M., and Worsnop, D. R.:
674 Real-time methods for estimating organic component mass concentrations from Aerosol
675 Mass Spectrometer data, *Environ. Sci. Technol.*, 45, 910-916, 10.1021/es102951k, 2011a.

676 Ng, N. L., Herndon, S. C., Trimborn, A., Canagaratna, M. R., Croteau, P. L., Onasch, T. B.,
677 Sueper, D., Worsnop, D. R., Zhang, Q., Sun, Y. L., and Jayne, J. T.: An Aerosol Chemical
678 Speciation Monitor (ACSM) for Routine Monitoring of the Composition and Mass
679 Concentrations of Ambient Aerosol, *Aerosol Sci. Technol.*, 45, 780-794,
680 10.1080/02786826.2011.560211, 2011b.

681 Paatero, P., and Tapper, U.: POSITIVE MATRIX FACTORIZATION - A NONNEGATIVE FACTOR
682 MODEL WITH OPTIMAL UTILIZATION OF ERROR-ESTIMATES OF DATA VALUES,
683 *Environmetrics*, 5, 111-126, 10.1002/env.3170050203, 1994.

684 Salcedo, D., Onasch, T. B., Dzepina, K., Canagaratna, M., Zhang, Q., Huffman, J., DeCarlo, P.,
685 Jayne, J., Mortimer, P., and Worsnop, D. R.: Characterization of ambient aerosols in
686 Mexico City during the MCMA-2003 campaign with Aerosol Mass Spectrometry: results
687 from the CENICA Supersite, *Atmos. Chem. Phys.*, 6, 925-946, 2006.

688 Seinfeld, J. H., and Pandis, S. N.: *Atmos. Chem. Phys.: from Air Pollution to Climate Change*,
689 Wiley, John & Sons, Incorporated, New York, 1203 pp., 2006.

690 Setyan, A., Song, C., Merkel, M., Knighton, W. B., Onasch, T. B., Canagaratna, M. R., Worsnop,

691 D. R., Wiedensohler, A., Shilling, J. E., and Zhang, Q.: Chemistry of new particle growth in
692 mixed urban and biogenic emissions – insights from CARES, *Atmos. Chem. Phys.*, 14,
693 6477-6494, 10.5194/acp-14-6477-2014, 2014.

694 Shen, X. J., Sun, J. Y., Zhang, Y. M., Wehner, B., Nowak, A., Tuch, T., Zhang, X. C., Wang, T. T.,
695 Zhou, H. G., Zhang, X. L., Dong, F., Birmili, W., and Wiedensohler, A.: First long-term study
696 of particle number size distributions and new particle formation events of regional
697 aerosol in the North China Plain, *Atmos. Chem. Phys.*, 11, 1565-1580,
698 10.5194/acp-11-1565-2011, 2011.

699 Sun, J., Zhang, Q., Canagaratna, M. R., Zhang, Y., Ng, N. L., Sun, Y., Jayne, J. T., Zhang, X.,
700 Zhang, X., and Worsnop, D. R.: Highly time- and size-resolved characterization of
701 submicron aerosol particles in Beijing using an Aerodyne Aerosol Mass Spectrometer,
702 *Atmos. Environ.*, 44, 131-140, 2010.

703 Sun, Y. L., Wang, Z., Dong, H., Yang, T., Li, J., Pan, X., Chen, P., and Jayne, J. T.: Characterization
704 of summer organic and inorganic aerosols in Beijing, China with an Aerosol Chemical
705 Speciation Monitor, *Atmos. Environ.*, 51, 250-259, 10.1016/j.atmosenv.2012.01.013,
706 2012.

707 Sun, Y. L., Wang, Z. F., Fu, P. Q., Yang, T., Jiang, Q., Dong, H. B., Li, J., and Jia, J. J.: Aerosol
708 composition, sources and processes during wintertime in Beijing, China, *Atmos. Chem.
709 Phys.*, 13, 4577-4592, 10.5194/acp-13-4577-2013, 2013.

710 Sun, Y. L., Jiang, Q., Wang, Z., Fu, P., Li, J., Yang, T., and Yin, Y.: Investigation of the
711 sources and evolution processes of severe haze pollution in Beijing in January
712 2013, *J. Geophys. Res.*, 119, 4380-4398, 10.1002/2014JD021641, 2014.

713 Takami, A., Miyoshi, T., Shimono, A., and Hatakeyama, S.: Chemical composition of fine
714 aerosol measured by AMS at Fukue Island, Japan during APEX period, *Atmos. Environ.*,
715 39, 4913-4924, 2005.

716 Takegawa, N., Miyakawa, T., Kuwata, M., Kondo, Y., Zhao, Y., Han, S., Kita, K., Miyazaki, Y.,
717 Deng, Z., Xiao, R., Hu, M., van Pinxteren, D., Herrmann, H., Hofzumahaus, A., Holland, F.,
718 Wahner, A., Blake, D. R., Sugimoto, N., and Zhu, T.: Variability of submicron aerosol
719 observed at a rural site in Beijing in the summer of 2006, *J. Geophys. Res.*, 114, D00G05,
720 10.1029/2008jd010857, 2009.

721 Tie, X., and Cao, J.: Aerosol pollution in China: Present and future impact on environment,
722 *Particuology*, 7, 426-431, <http://dx.doi.org/10.1016/j.partic.2009.09.003>, 2009.

723 Topping, D., Coe, H., McFiggans, G., Burgess, R., Allan, J., Alfarra, M. R., Bower, K., Choularton,
724 T. W., Decesari, S., and Facchini, M. C.: Aerosol chemical characteristics from sampling
725 conducted on the Island of Jeju, Korea during ACE Asia, *Atmos. Environ.*, 38, 2111-2123,
726 10.1016/j.atmosenv.2004.01.022, 2004.

727 Ulbrich, I. M., Canagaratna, M. R., Zhang, Q., Worsnop, D. R., and Jimenez, J. L.:
728 Interpretation of organic components from Positive Matrix Factorization of aerosol mass
729 spectrometric data, *Atmos. Chem. Phys.*, 9, 2891-2918, 2009.

730 Wan, X., Kang, S. C., Wang, Y. S., Xin, J. Y., Liu, B., Guo, Y. H., Wen, T. X., Zhang, G. S., and Cong,
731 Z. Y.: Size distribution of carbonaceous aerosols at a high-altitude site on the central
732 Tibetan Plateau (Nam Co Station, 4730 m a.s.l.), *Atmospheric Research*, 153, 155-164,
733 10.1016/j.atmosres.2014.08.008, 2015.

734 Wang, Z. B., Hu, M., Sun, J. Y., Wu, Z. J., Yue, D. L., Shen, X. J., Zhang, Y. M., Pei, X. Y., Cheng, Y.

735 F., and Wiedensohler, A.: Characteristics of regional new particle formation in urban and
736 regional background environments in the North China Plain, *Atmos. Chem. Phys.*, 13,
737 12495-12506, 10.5194/acp-13-12495-2013, 2013a.

738 Wang, Z. B., Hu, M., Wu, Z. J., Yue, D. L., He, L. Y., Huang, X. F., Liu, X. G., and Wiedensohler, A.:
739 Long-term measurements of particle number size distributions and the relationships
740 with air mass history and source apportionment in the summer of Beijing, *Atmos. Chem.*
741 *Phys.*, 13, 10159-10170, 10.5194/acp-13-10159-2013, 2013b.

742 Weber, R. J., Marti, J. J., McMurry, P. H., Eisele, F. L., Tanner, D. J., and Jefferson, A.:
743 Measurements of new particle formation and ultrafine particle growth rates at a clean
744 continental site, *J. Geophys. Res.*, 102, 4375, 10.1029/96jd03656, 1997.

745 Wiedensohler, A., Cheng, Y. F., Nowak, A., Wehner, B., Achtert, P., Berghof, M., Birmili, W., Wu,
746 Z. J., Hu, M., Zhu, T., Takegawa, N., Kita, K., Kondo, Y., Lou, S. R., Hofzumahaus, A.,
747 Holland, F., Wahner, A., Gunthe, S. S., Rose, D., Su, H., and Poschl, U.: Rapid aerosol
748 particle growth and increase of cloud condensation nucleus activity by secondary aerosol
749 formation and condensation: A case study for regional air pollution in northeastern
750 China, *J. Geophys. Res.-Atmos.*, 114, D00g08,10.1029/2008jd010884, 2009.

751 Wu, Z., Hu, M., Liu, S., Wehner, B., Bauer, S., Maßling, A., Wiedensohler, A., Petäjä, T., Dal
752 Maso, M., and Kulmala, M.: New particle formation in Beijing, China: Statistical analysis
753 of a 1-year data set, *J. Geophys. Res.*, 112, 10.1029/2006jd007406, 2007.

754 Xu, J., Zhang, Q., Chen, M., Ge, X., Ren, J., and Qin, D.: Chemical composition, sources, and
755 processes of urban aerosols during summertime in northwest China: insights from
756 high-resolution aerosol mass spectrometry, *Atmos. Chem. Phys.*, 14, 12593-12611,
757 10.5194/acp-14-12593-2014, 2014a.

758 Xu, J. Z., Wang, Z. B., Yu, G. M., Qin, X., Ren, J. W., and Qin, D.: Characteristics of water
759 soluble ionic species in fine particles from a high altitude site on the northern boundary
760 of Tibetan Plateau: Mixture of mineral dust and anthropogenic aerosol, *Atmos. Res.*, 143,
761 43-56, 10.1016/j.atmosres.2014.01.018, 2014b.

762 Xu, J. Z., Zhang, Q., Wang, Z. B., Yu, G. M., Ge, X. L., and Qin, X.: Chemical composition and
763 size distribution of summertime PM_{2.5} at a high altitude remote location in the
764 northeast of the Qinghai–Xizang (Tibet) Plateau: insights into aerosol sources and
765 processing in free troposphere, *Atmos. Chem. Phys.*, 15, 5069-5081,
766 10.5194/acp-15-5069-2015, 2015.

767 Yue, D. L., Hu, M., Zhang, R. Y., Wang, Z. B., Zheng, J., Wu, Z. J., Wiedensohler, A., He, L. Y.,
768 Huang, X. F., and Zhu, T.: The roles of sulfuric acid in new particle formation and growth
769 in the mega-city of Beijing, *Atmos. Chem. Phys.*, 10, 4953-4960,
770 10.5194/acp-10-4953-2010, 2010.

771 Zhang, Q., Worsnop, D. R., Canagaratna, M. R., and Jimenez, J. L.: Hydrocarbon-like and
772 oxygenated organic aerosols in Pittsburgh: Insights into sources and processes of organic
773 aerosols, *Atmos. Chem. Phys.*, 5, 3289-3311, 2005.

774 Zhang, Q., Jimenez, J. L., Canagaratna, M. R., Allan, J. D., Coe, H., Ulbrich, I., Alfarra, M. R.,
775 Takami, A., Middlebrook, A. M., Sun, Y. L., Dzepina, K., Dunlea, E., Docherty, K., DeCarlo, P.
776 F., Salcedo, D., Onasch, T., Jayne, J. T., Miyoshi, T., Shimojo, A., Hatakeyama, S., Takegawa,
777 N., Kondo, Y., Schneider, J., Drewnick, F., Borrmann, S., Weimer, S., Demerjian, K.,
778 Williams, P., Bower, K., Bahreini, R., Cottrell, L., Griffin, R. J., Rautiainen, J., Sun, J. Y.,

779 Zhang, Y. M., and Worsnop, D. R.: Ubiquity and dominance of oxygenated species in
780 organic aerosols in anthropogenically-influenced Northern Hemisphere midlatitudes,
781 *Geophys. Res. Lett.*, 34, L13801,10.1029/2007gl029979, 2007a.

782 Zhang, Q., Jimenez, J. L., Worsnop, D. R., and Canagaratna, M.: A case study of urban particle
783 acidity and its effect on secondary organic aerosol, *Environ. Sci. Technol.*, 41, 3213-3219,
784 2007b.

785 Zhang, Q., Jimenez, J. L., Canagaratna, M. R., Ulbrich, I. M., Ng, N. L., Worsnop, D. R., and Sun,
786 Y.: Understanding atmospheric organic aerosols via factor analysis of aerosol mass
787 spectrometry: a review, *Anal. Bioanal. Chem.*, 401, 3045-3067,
788 10.1007/s00216-011-5355-y, 2011a.

789 Zhang, Y. J., Tang, L. L., Wang, Z., Yu, H. X., Sun, Y. L., Liu, D., Qin, W., Canonaco, F., Prévôt, A. S.
790 H., Zhang, H. L., and Zhou, H. C.: Insights into characteristics, sources, and evolution of
791 submicron aerosols during harvest seasons in the Yangtze River delta region, China,
792 *Atmos. Chem. Phys.*, 15, 1331-1349, 10.5194/acp-15-1331-2015, 2015.

793 Zhang, Y. M., Zhang, X. Y., Sun, J. Y., Lin, W. L., Gong, S. L., Shen, X. J., and Yang, S.:
794 Characterization of new particle and secondary aerosol formation during summertime in
795 Beijing, China, *Tellus B*, 63, 382-394, 10.1111/j.1600-0889.2011.00533.x, 2011b.

796 Zhang, Y. M., Zhang, X. Y., Sun, J. Y., Hu, G. Y., Shen, X. J., Wang, Y. Q., Wang, T. T., Wang, D. Z.,
797 and Zhao, Y.: Chemical composition and mass size distribution of PM₁ at an
798 elevated site in central east China, *Atmos. Chem. Phys.*, 14, 12237-12249,
799 10.5194/acp-14-12237-2014, 2014.

800 Zhao, Z. Z., Cao, J. J., Shen, Z. X., Xu, B. Q., Zhu, C. S., Chen, L. W. A., Su, X. L., Liu, S. X., Han, Y.
801 M., Wang, G. H., and Ho, K. F.: Aerosol particles at a high-altitude site on the Southeast
802 Tibetan Plateau, China: Implications for pollution transport from South Asia, *J. Geophys.*
803 *Res.-Atmos.*, 118, 11360-11375, 10.1002/jgrd.50599, 2013.

804 **Tables**

805 Table 1. A summary of average mass concentrations ($\mu\text{g m}^{-3}$) of PM_{10} species during
 806 five episodes and the entire study. The 30 min detection limit (DLs) of the ACSM is
 807 also shown (Sun et al., 2012).

808

	Org	SO ₄	NO ₃	NH ₄	Cl	BC	PM ₁₀
Entire Study	4.9	3.2	1.2	1.4	0.14	0.51	11.4
Clean1	1.2	1.3	0.25	0.58	0.02	0.22	3.6
Clean2	1.8	1.3	0.24	0.45	0.03	-	3.8
Ep1	19.1	2.1	2.7	1.4	0.53	1.4	27.2
Ep2	6.3	5.9	2.0	2.6	0.18	0.57	17.6
Ep3	10.8	6.0	2.9	2.6	0.39	1.0	23.7
DLs	0.54	0.07	0.06	0.25	0.03		

809

810

811 **Figure Captions:**

812 ~~Figure 1. Map of the sampling site (Menyuan, Qinghai). Also shown is the chemical~~
813 ~~composition of submicron aerosols (NR-PM₁ + BC if it was available) measured at~~
814 ~~selected rural/remote sites in East Asia except Lanzhou, an urban site in northwest~~
815 ~~China. The two dotted blue lines are used to guide eyes for the three rural/remote~~
816 ~~regions from the west to the east. The detailed information of the sampling sites is~~
817 ~~presented in Table S1.~~
818 ~~Figure 1. Map of the sampling site (Menyuan, Qinghai). Also~~
819 ~~shown is the chemical composition of submicron aerosols measured at selected~~
820 ~~rural/remote sites in East Asia except Lanzhou, an urban site in northwest China. The~~
~~detailed information of the sampling sites is presented in Table S1.~~

821 Figure 2. Comparison of the mass concentrations of PM₁ (NR-PM₁ +BC) measured
822 by the ACSM and Aethalometer with that by the SMPS ($D_m = 12 - 478$ nm): (a) time
823 series and (b) scatter plot.

824 Figure 3. Time series of (a-c) meteorological variables including T (temperature), RH
825 (relative humidity), Precip. (precipitation), WS (wind speed), WD (wind direction),
826 and Vis (visibility), (d) mass concentrations and (e) mass fractions of PM₁ species .
827 The pie charts show the average chemical composition of PM₁ for five episodes.

828 Figure 4. Average diurnal cycles of (a) mass concentration; (b) mass fraction of PM₁
829 species; (c) ratios of aerosol species to CO, and (d) gaseous species. The local sunrise
830 and sunset was around 7:00 and 19:00, respectively.

831 Figure 5. (a) Mass spectra and (b) time series of mass concentrations of BBOA and
832 OOA. The standard average mass spectra of BBOA and OOA in Ng et al. (2011) are
833 also shown for the comparison. The pie chart in (b) shows the average composition of
834 OA for the entire study.

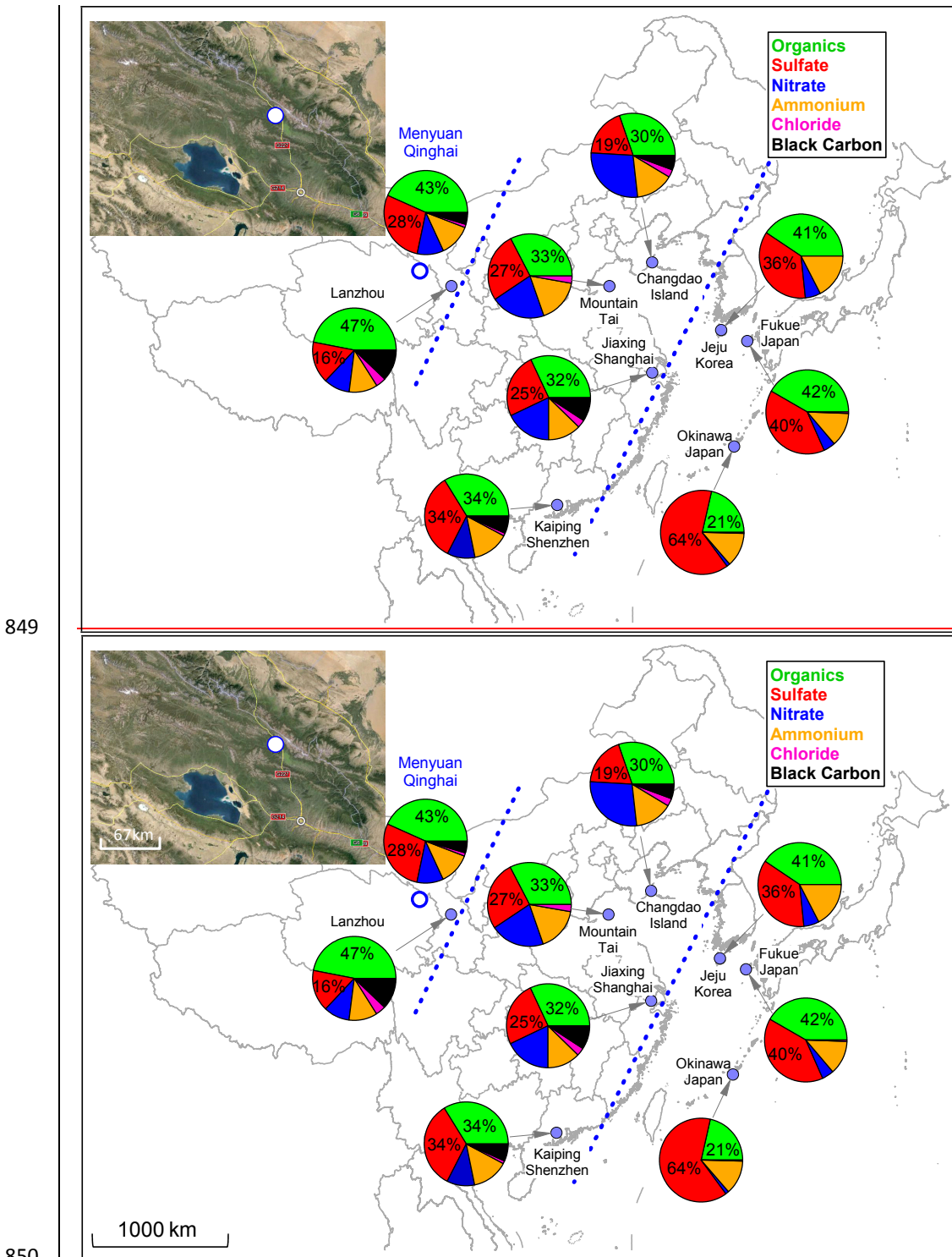
835 Figure 6. Scatter plot of OOA versus SO₄ during BB and NBB periods. The data
836 points are color coded by BBOA concentrations. The pie chart shows the average
837 composition of OA with post-processed OOA (= OOA - SO₄ × [OOA/SO₄]_{NBB}).

838 Figure 7. (a) The evolution of particle number size distributions; (b) average particle
839 number size distributions during NPE and non-NPE; (c,d) time series and diurnal
840 cycles of particle number concentrations for three different sizes. The log-normal
841 distribution fitting of each mode is shown in (b) as dash lines. The sunrise time was
842 around 7:00.

843 Figure 8. Diurnal evolution of particle size distributions, aerosol composition, gaseous
844 precursors, and the ratios of aerosol species to CO during (a) NPE and (b) non-NPE.
845 The sunrise time was approximately 7:00.

846 Figure 9. (a) Time series of OOA/PM₁, particle growth rates, and average chemical

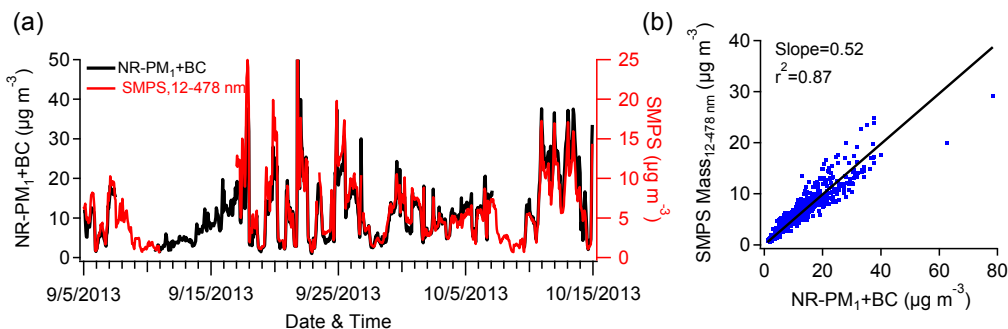
847 composition during particle growth periods; (b) correlation of growth rate with
 848 OOA/PM₁. The data points are color coded by the PM₁ mass concentration.



850 Figure 1. Map of the sampling site (Menyuan, Qinghai). Also shown is the
 851 chemical composition of submicron aerosols (NR-PM₁ + BC if it was available)
 852 measured at selected rural/remote sites in East Asia except Lanzhou, an urban site in
 853

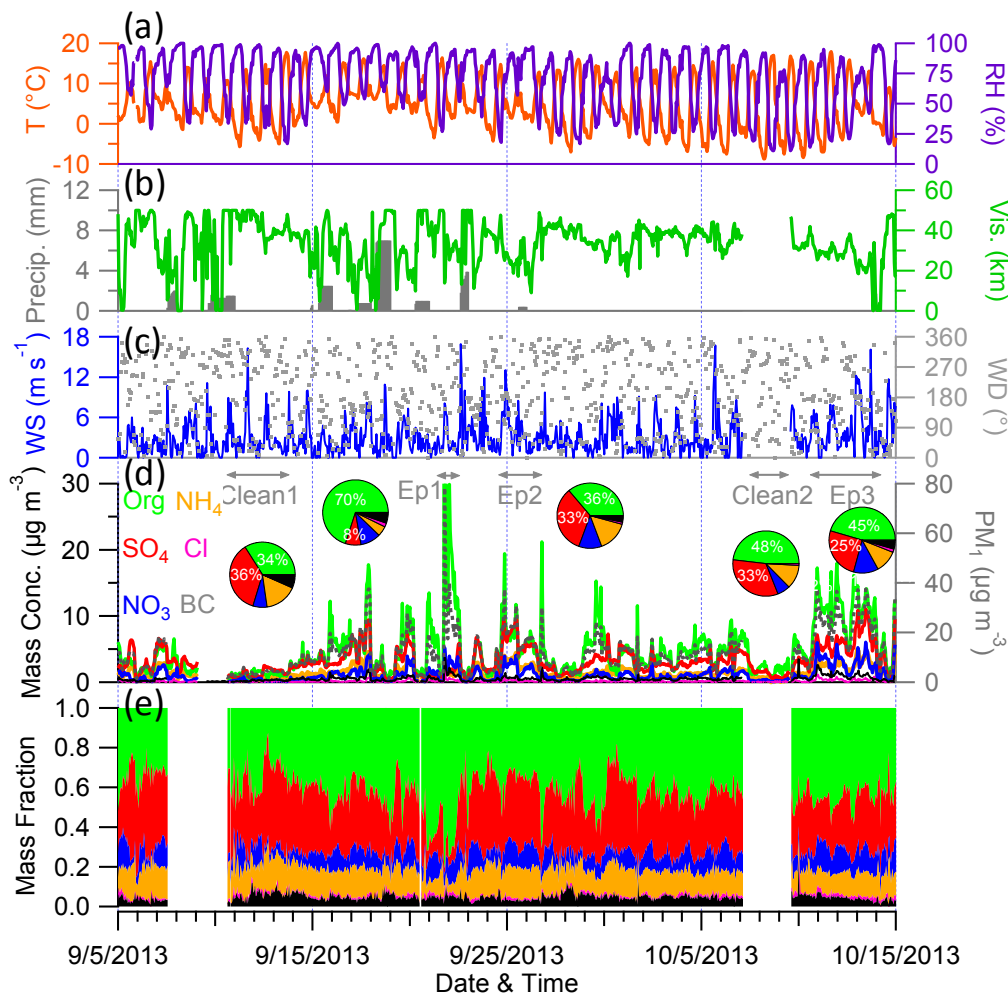
854 northwest China. The two dotted blue lines are used to guide eyes for the three
 855 rural/remote regions from the west to the east. The detailed information of the
 856 sampling sites is presented in Table S1.

857
 858



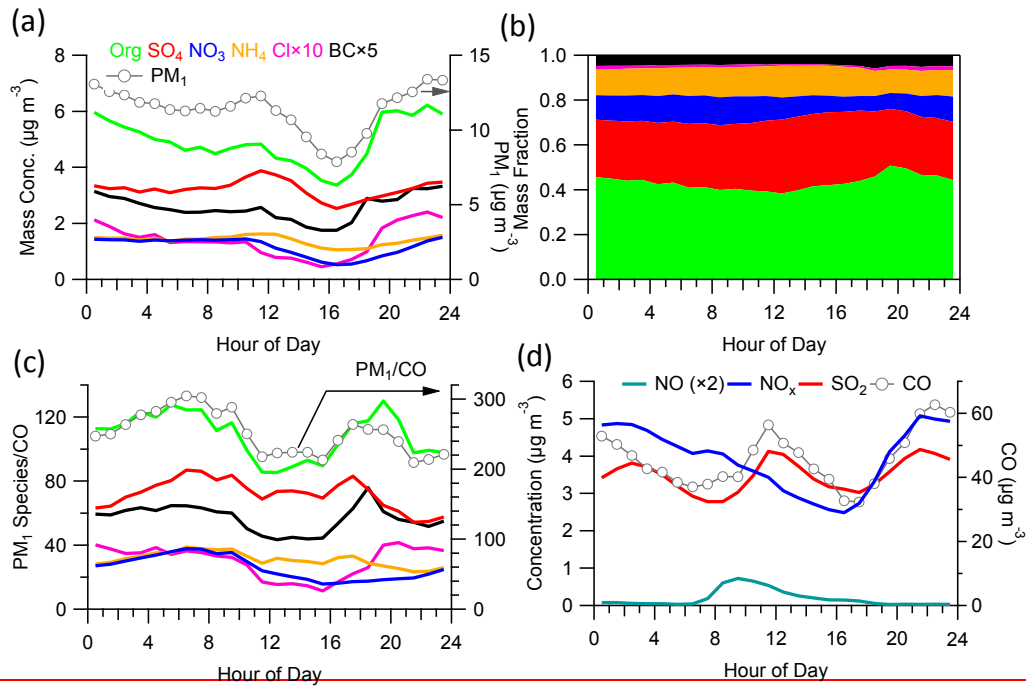
859

860 Figure 2. Comparison of the mass concentrations of PM₁ (NR-PM₁ +BC) measured
 861 by the ACSM and Aethalometer with that by the SMPS ($D_m = 12 - 478$ nm): (a) time
 862 series and (b) scatter plot.

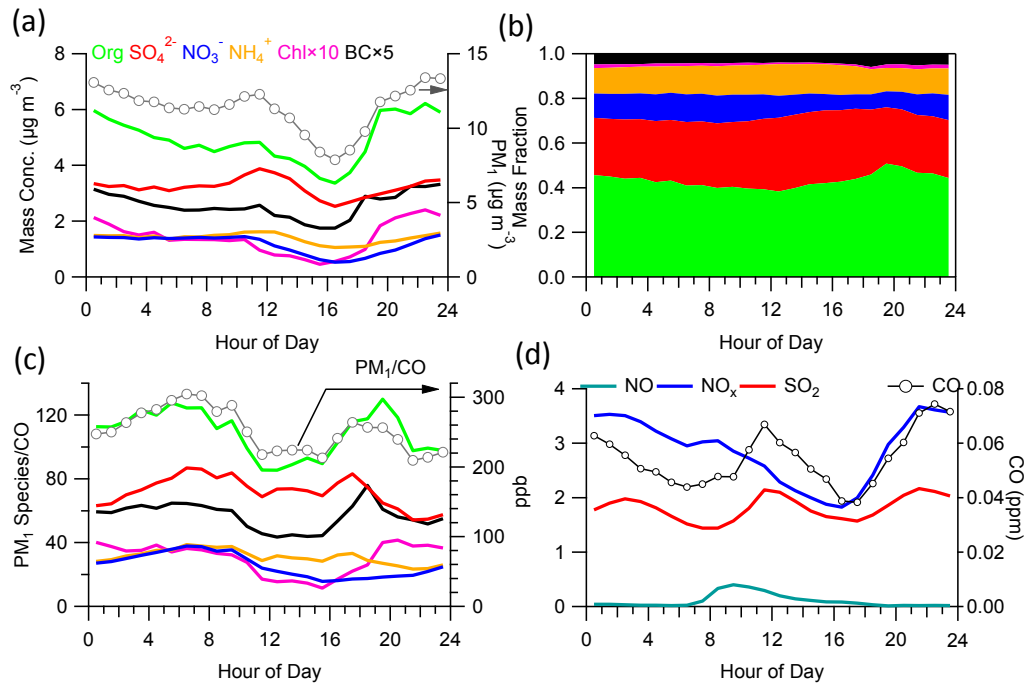


863

864 Figure 3. Time series of (a-c) meteorological variables including T (temperature), RH
 865 (relative humidity), Precip. (precipitation), WS (wind speed), WD (wind direction),
 866 and Vis (visibility), (d) mass concentrations and (e) mass fractions of PM₁ species .
 867 The pie charts show the average chemical composition of PM₁ for five episodes.

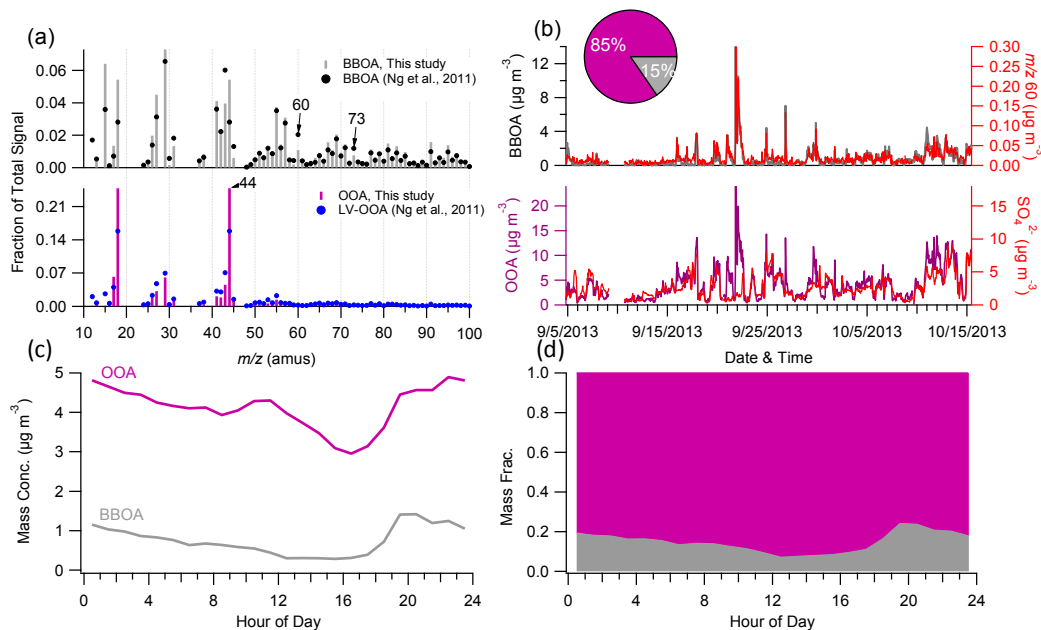


868



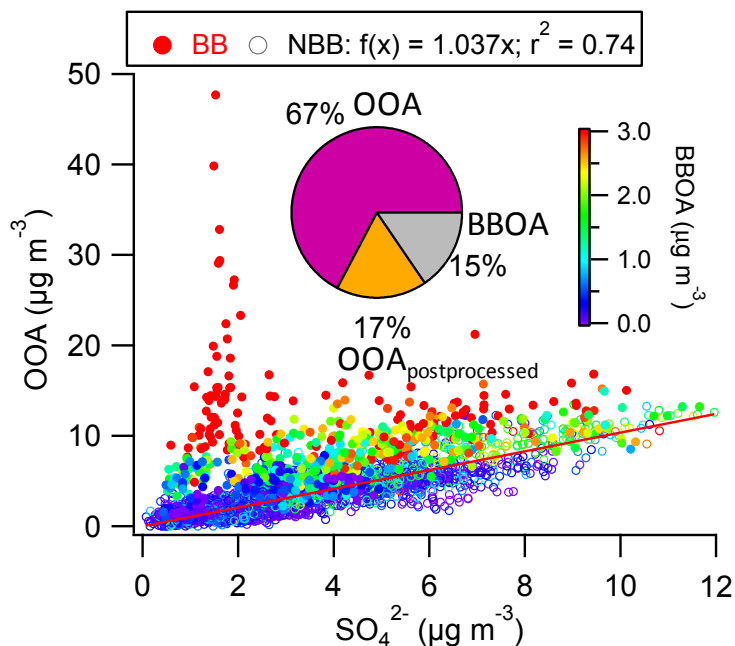
869

870 Figure 4. Average diurnal cycles of (a) mass concentration; (b) mass fraction of PM₁
 871 species; (c) ratios of aerosol species to CO, and (d) gaseous species. The local sunrise
 872 and sunset was around 7:00 and 19:00, respectively.



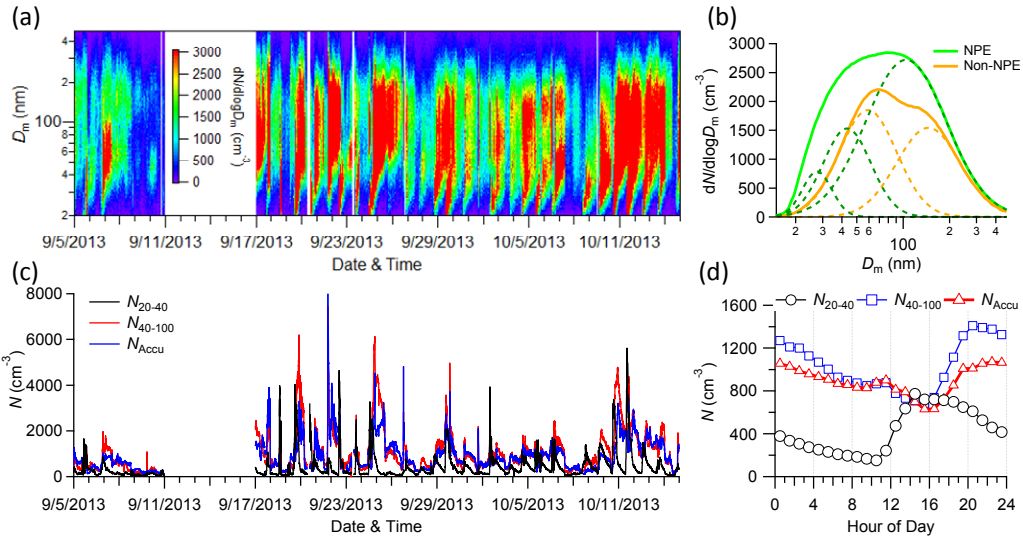
873

874 Figure 5. (a) Mass spectra and (b) time series of mass concentrations of BBOA and
 875 OOA, (c) and (d) show the average diurnal cycles of BBOA and OOA. In addition,
 876 the standard average mass spectra of BBOA and OOA in Ng et al. (2011) are also
 877 shown in (a) for the comparison. The pie chart in (b) shows the average composition
 878 of OA for the entire study.



879

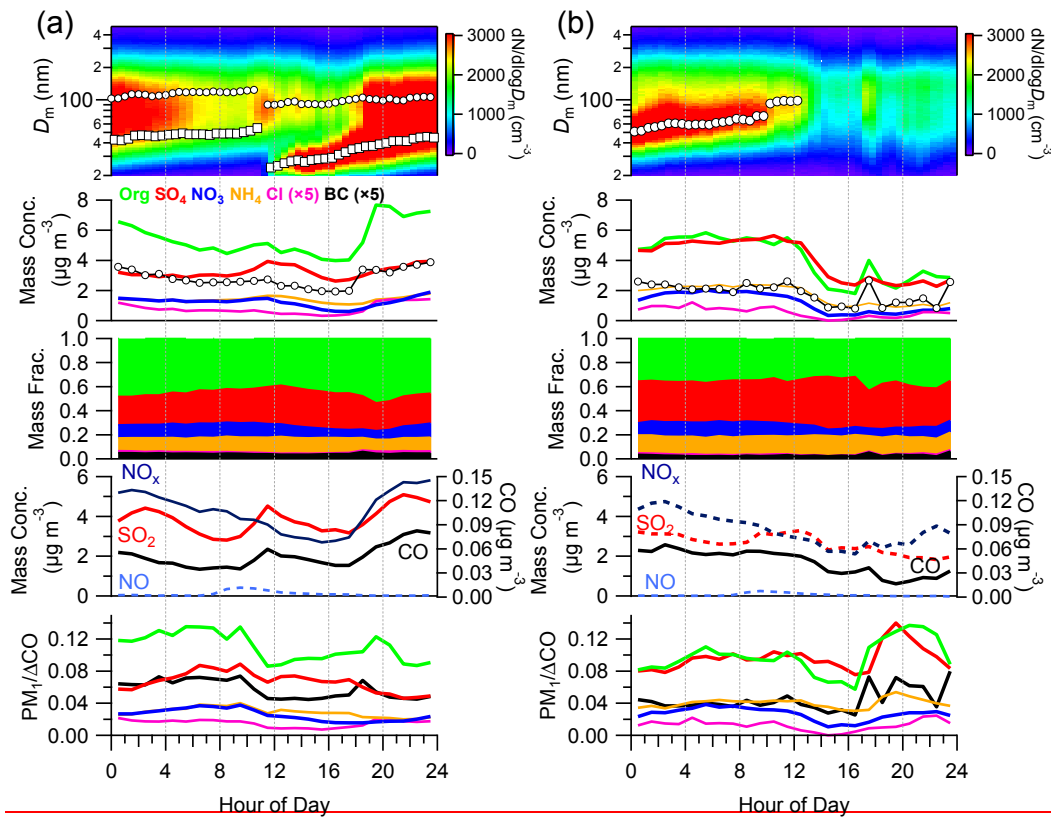
880 Figure 6. Scatter plot of OOA versus SO_4 during BB and NBB periods. The data
 881 points are color coded by BBOA concentrations. The pie chart shows the average
 882 composition of OA with post-processed OOA ($= \text{OOA} - \text{SO}_4 \times [\text{OOA}/\text{SO}_4]_{\text{NBB}}$).



883

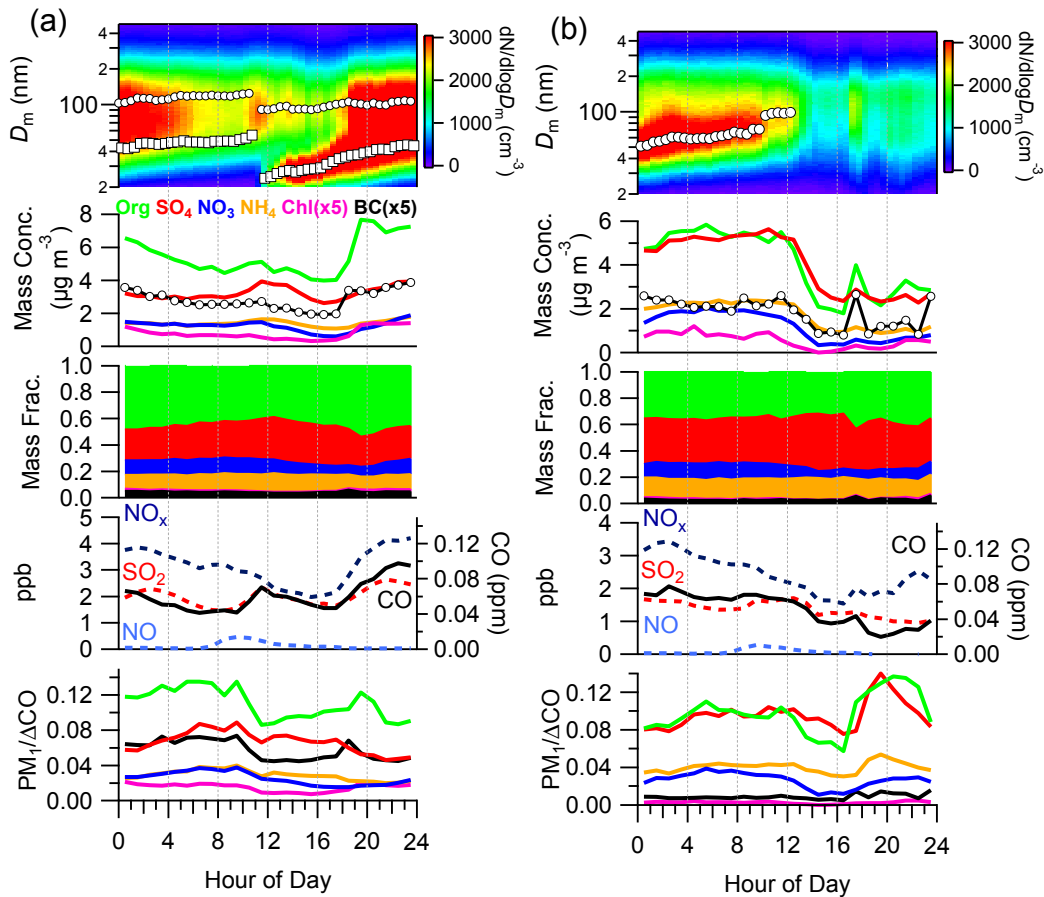
884

885 Figure 7. (a) The evolution of particle number size distributions; (b) average particle
 886 number size distributions during NPE and non-NPE; (c,d) time series and diurnal
 887 cycles of particle number concentrations for three different sizes. The log-normal
 888 distribution fitting of each mode is shown in (b) as dash lines. The sunrise time was
 889 around 7:00.



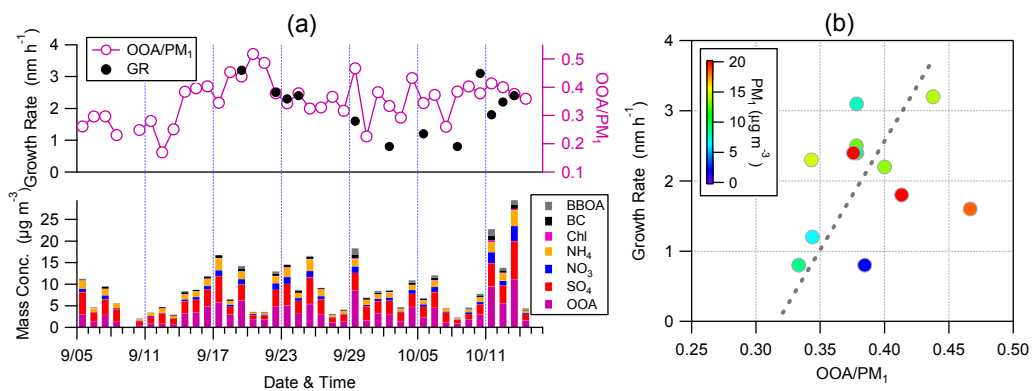
890

891



892

893 Figure 8. Diurnal evolution of particle size distributions, aerosol composition, gaseous
 894 precursors, and the ratios of aerosol species to CO during (a) NPE and (b) non-NPE.
 895 The sunrise time was approximately 7:00.



896

897 Figure 9. (a) Time series of OOA/PM₁, particle growth rates, and average chemical
 898 composition during particle growth periods; (b) correlation of growth rate with
 899 OOA/PM₁. The data points are color coded by the PM₁ mass concentration.